N82-16046

SUMMARY OF THEORETICAL CONSIDERATIONS AND WIND TUNNEL TESTS OF AN AERODYNAMIC SPOILER FOR STALL PROOFING A GENERAL AVIATION AIRPLANE

Prepared by:

Howard L. Chevalier

TEXAS A&M UNIVERSITY

COLLEGE STATION, TEXAS

January, 1981

NASA Research Grant NSG - 1407

NASA Langley Research Center

Final Report

Abstract

An airplane stall proofing system utilizing a spoiler has been investigated for application on a low wing airplane representative of typical general aviation airplane. Tests of the full scale airplane were conducted in the NASA Langley 30 x 60 foot full scale wind tunnel. The test velocity was 86 feet per second, corresponding to a Reynolds number of 2.20×10^6. This report shows the stall proofing capability of the spoiler and verifies a theoretical approach to the design of the spoiler and analysis of the spoiler's contribution to the airplane's trim and longitudinal stability. Controlled spoiler deployment in a narrow angle of attack range, 4 degrees, immediately preceding the stall angle will stall proof the airplane. The results of this investigation also show some of the limitations of small scale tests and the need for full scale flight tests to determine spoiler deployment rate for good handling qualities.

NOMENCLATURE

bhp	Brake horsepower
c	Chord length, ft
c.g.	Center of gravity, % c
C_{h_e}	Elevator hinge moment coefficient
C_L	Airplane lift coefficient
$C_{L_{MAX}}$	Maximum obtainable lift coefficient
C_{L_T}	Tail lift coefficient
C_M	Airplane pitching moment coefficient
C_{M_0}	Airplane pitching moment coefficient at zero lift
C_{M_T}	Airplane pitching moment coefficient due to the tail
C_{M_α}	Slope of the C_M vs α curve
$C_{M_{\delta_e}}$	Slope of the C_M vs δ_e curve
h/c	The ratio of spoiler height to the tail mean geometric chord
l_t	Distance from the center of gravity to the aerodynamic center of the tail, ft
m_T	Lift curve slope of the tail, per degree
m_W	Lift curve slope of the wing, per degree
R_N	Reynolds number

NOMENCLATURE (continued)

$\bar{V}$	Tail volume
α	Angle of attack, degree
α_a	Angle of attack at which spoiler activation begins
α_{L_0}	Angle of attack which produces zero net lift
α_s	Angle of attack at which the airplane stalls
δ_e	Elevator deflection angle, degree
ϵ	Wing downwash angle at the tail, degree
η_T	Tail efficiency factor

Introduction

Airplane stall/spin accidents account for a major portion of the fatal and nonfatal accidents in general aviation flying each year. Through the years, many attempts have been made to solve this problem. Two basic approaches have been taken in an effort to obtain a solution. One approach has been to design a stall proof wing. The second effort has been to alter the control system of the airplane in some manner to limit the airplane's angle of attack to an angle below stall. A third approach formed by the authors several years ago, and recently refined, alters both the stability and control of the aircraft at high angles of attack to produce a stall proof aircraft.[1,2,3,4] In this approach, two fundamental requirements must be met; the airplane must automatically trim at an angle of attack below the stall angle, and there should be a restoring moment at this trim condition which cannot be overridden by control inputs from the pilot. This stabilizing moment should be such that it increases at high angles of attack and at the maximum trim angle of attack makes the rate of change of stabilizing moment due to the aerodynamics of the aircraft greater than that of the rate of change of pitch up moment produced by control or gust inputs. This report shows that a simple stability augmentation system, a spoiler mounted on the lower surface of the horizontal stabilizer, can meet these requirements.

A full scale general aviation aircraft was tested in the NASA Langley 30 x 60 foot wind tunnel using a spoiler. Configuration

requirements for the full scale tests were based on theoretical analysis of the spoiler effects, small scale testing in the NASA Langley 12 foot low speed wind tunnel and tests of a semi-span of the airplane's horizontal tail in the Texas A&M University's 7 x 10 foot low speed wind tunnel.

This report presents the results obtained from the full scale tests and show that they provide "proof of concept" for the theory developed in Reference [3]. It will also be shown that, if used judiciously, the data provided by the wind tunnel tests of the scale model and horizontal tail alone can provide the basis for preliminary design of the full scale spoiler system.

Background

The authors have been actively involved in developing a stall proofing system utilizing a spoiler as the control surface for the last 10 years. Early flight testing of such systems was essentially by trial and error and met with only limited success.[1,2] This was because most aerodynamic effects of the spoiler were not known, and the system could not be studied using theoretical approaches.

Wind tunnel tests of a 1/5 scale model of the full sized aircraft[4], and of a full scale semi-span horizontal tail[5], showed that the spoiler could provide the necessary stability and control authority with minimum complications in terms of installation and actuation. They also provided the necessary data from which to develop a theoretical approach for analyzing the effects and contributions of the spoiler to longitudinal stability. This analysis is treated in detail in References 3 and 4. In the analysis, the effects of the elevator and spoiler on each other were assumed to be negligible and as a result the spoiler's contribution to the aircraft's longitudinal pitching moment became a separate, independent term in the pitching moment coefficient equation:

$$C_{M_{c.g.}} = -C_{M_{\delta_e}} \delta_e + C_{M_0} + \frac{\partial C_M}{\partial C_L} C_L$$

$$+ 2m_T \nabla_{n_T} \frac{\partial \alpha_{L_0}}{\partial h/c} \frac{\partial h/c_\alpha}{\partial \alpha} \qquad (1)$$

In the spoiler contribution term, the last term in Equation (1), h/c is the ratio of spoiler height to horizontal tail chord and the effect of spoiler deployment is a shift in the angle of zero lift of the tail. Selection of a proper program for $\frac{\partial h/c}{\partial \alpha}$ would provide the trim and stability required to prevent stall. Figure 1 is an idealized C_M vs. angle of attack curve for a given elevator deflection such that the aircraft would normally trim (C_M=0) above the stall angle of attack. The dashed line in Figure 1 shows a stall proof case. Figure 2 depicts the programmed spoiler deployment schedule for such an aircraft. The spoiler is only deployed in the 4° angle of attack range just below the stall. At angles of attack below that, the spoiler remains closed and the last term in Equation (1) is zero. The third term in Equation (1) is then the only stability contribution. The equation for the curve in Figure 2 is:

$$h/c = 2.37 \times 10^{-3} (\Delta\alpha)^{2.4}$$

$$\text{where } \Delta\alpha = \alpha - \alpha_a \qquad (2)$$

The spoiler deployment schedule developed in References 3 and 4, described by Equation (2), results in the nonlinear pitching moment curve shown as the dashed line in Figure 1. The result of this deployment schedule is that the aircraft trims (reaches equilibrium) below the stall angle of attack and the slope of the curve becomes increasingly negative as stall is approached, producing an increasingly stable aircraft.

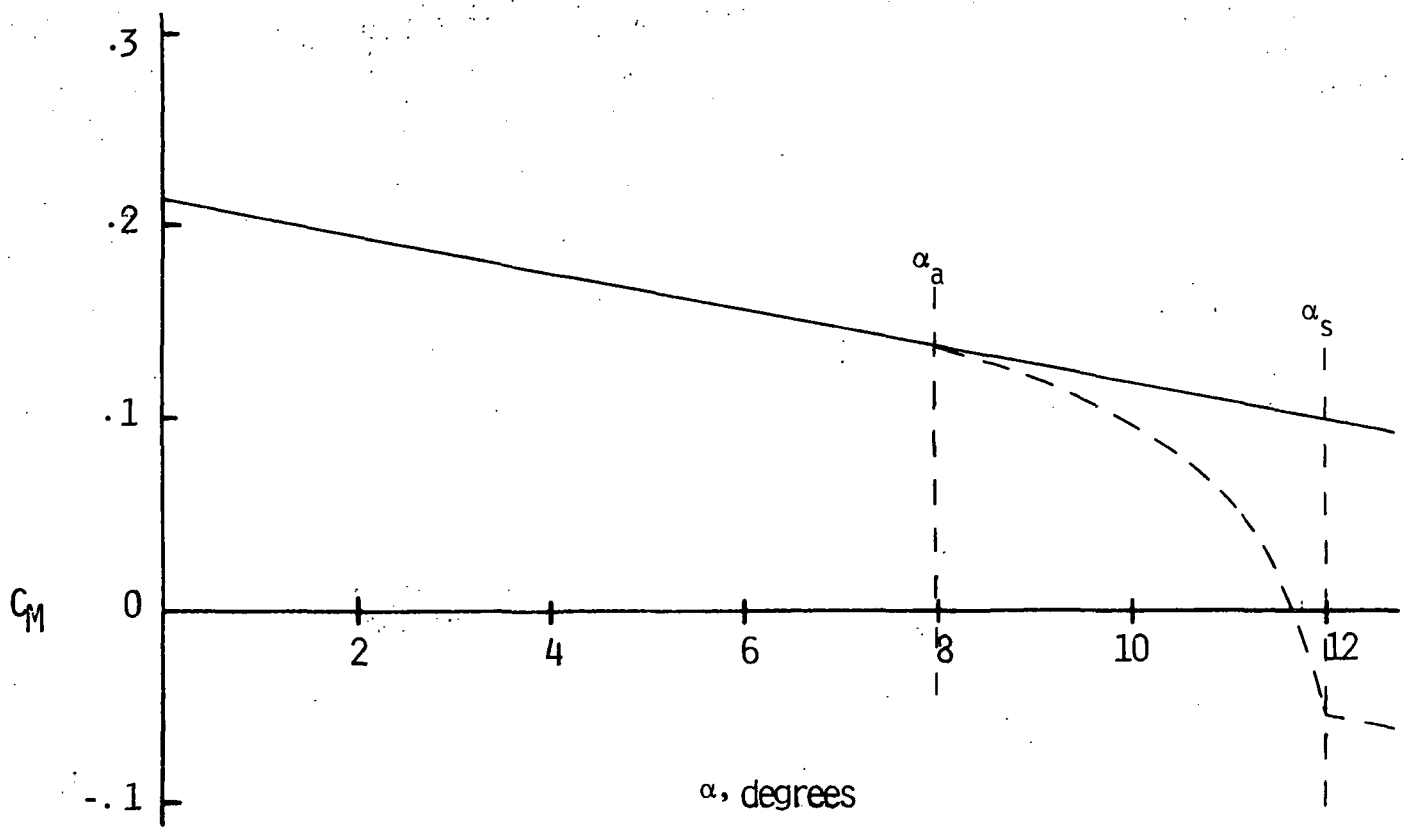

Figure 1. Theoretical Variation of Pitching Moment Coefficient with Angle of Attack

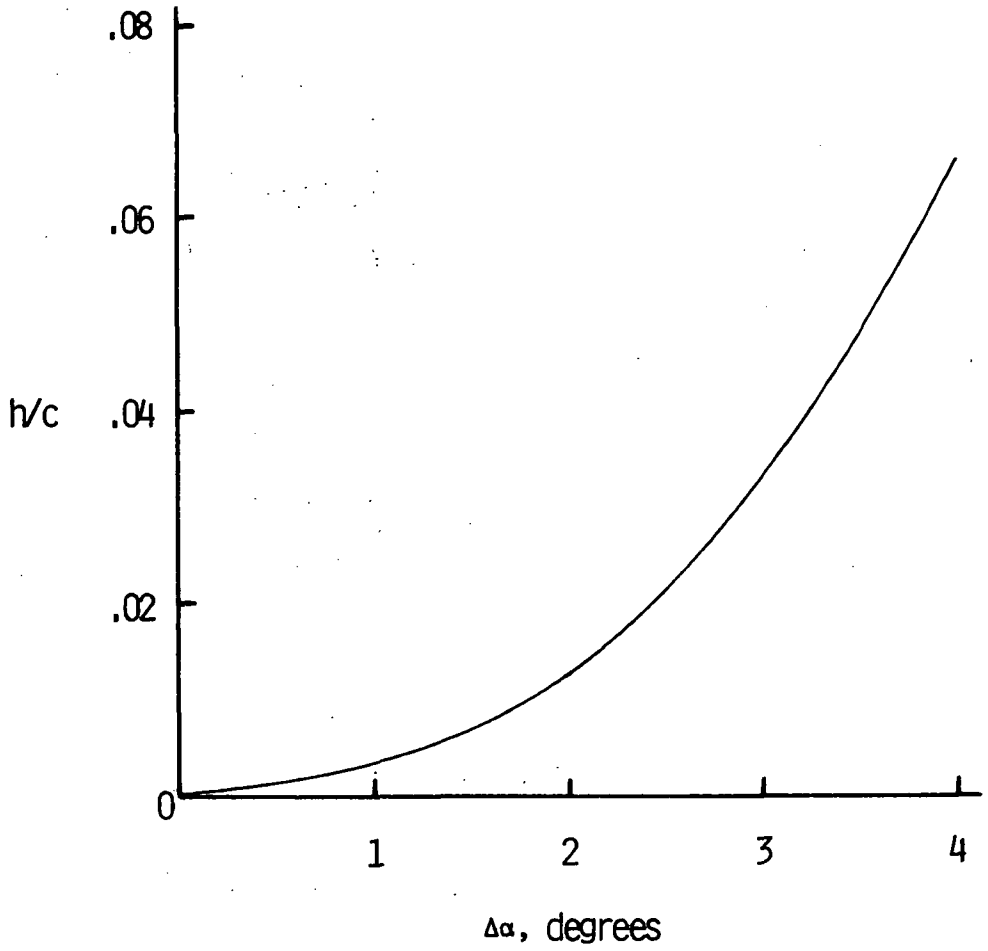

Figure 2. Variation of Spoiler Height with Angle of Attack

Selection of both the angle of attack range for the active spoiler and the exponent in Equation (2) must remain somewhat arbitrary until flight tests are conducted to evaluate the airplane's handling characteristics. Equation (2) is based on such considerations as a smooth transition from basic to spoiler augmented stability and the desired slope, C_{M_α}, at trim.

Model Description

The dimensions of the airplane used in this test are shown in Figure 3. The aircraft is representative of a single engine low wing general aviation airplane. Figure 4 shows a photograph of the airplane mounted in the test section of the NASA 30 x 60 foot wind tunnel.

A controllable spoiler was mounted on the underside of the horizontal stabilizer just forward of the elevator hinge line and of the same span. The spoiler was mounted flush against the stabilizer skin in the fully retracted position. The spoiler was hinged at its forward edge and could be deployed through an arc from zero to 90 degrees. Figure 5 illustrates the spoiler mounting and operation.

The spoiler chord was 2 inches. The mean geometric chord of the horizontal stabilizer was 30.8" and the maximum h/c was 0.065. For most tests, the maximum spoiler extension was 60°, corresponding to an h/c of 0.056.

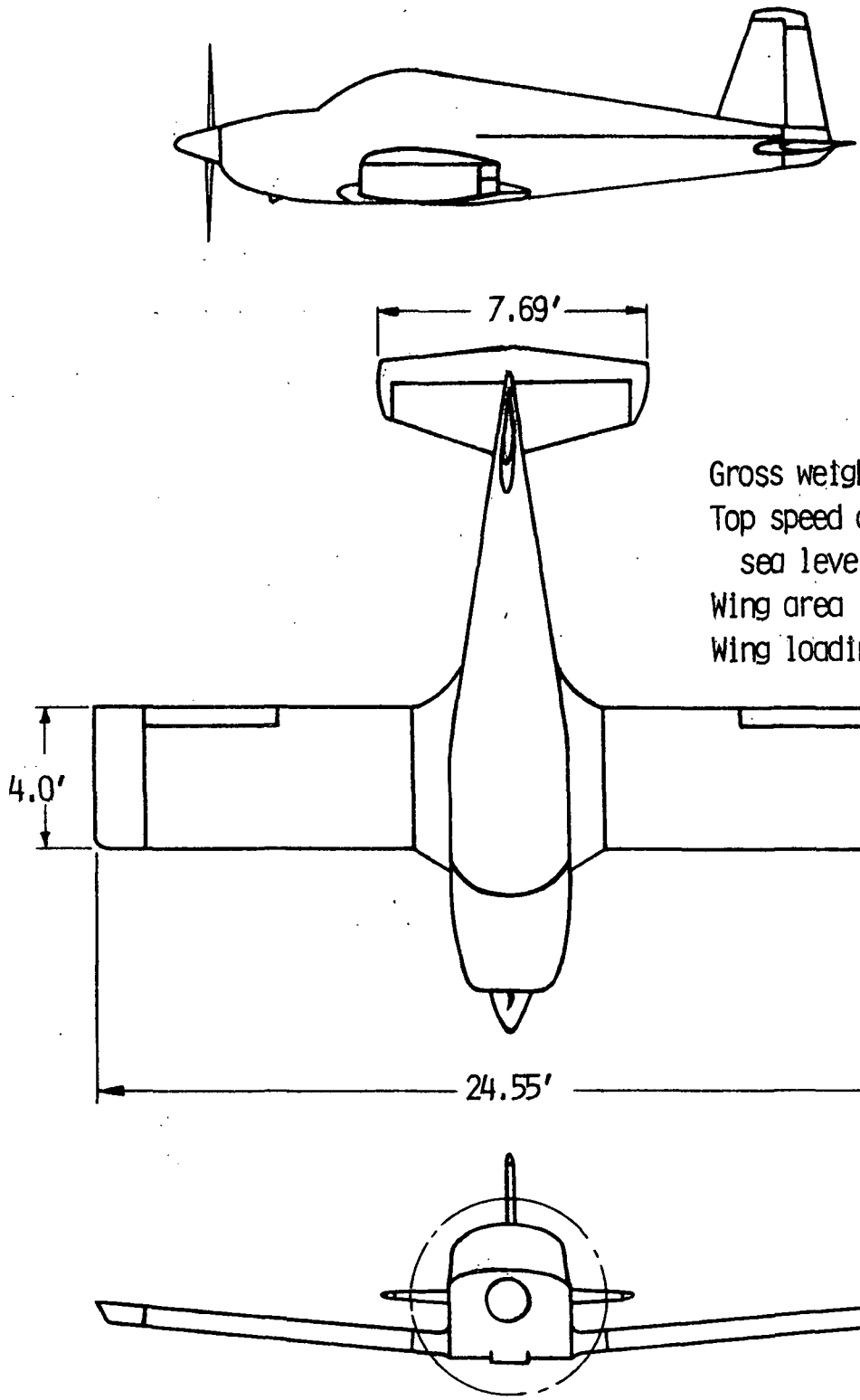

Gross weight . . . 1500 lbs.
Top speed at
sea level . . . 144 MPH
Wing area . . . 98.0 sq. ft.
Wing loading . . . 15.27 lbs./
sq. ft.

Figure 3. Airplane Dimensions

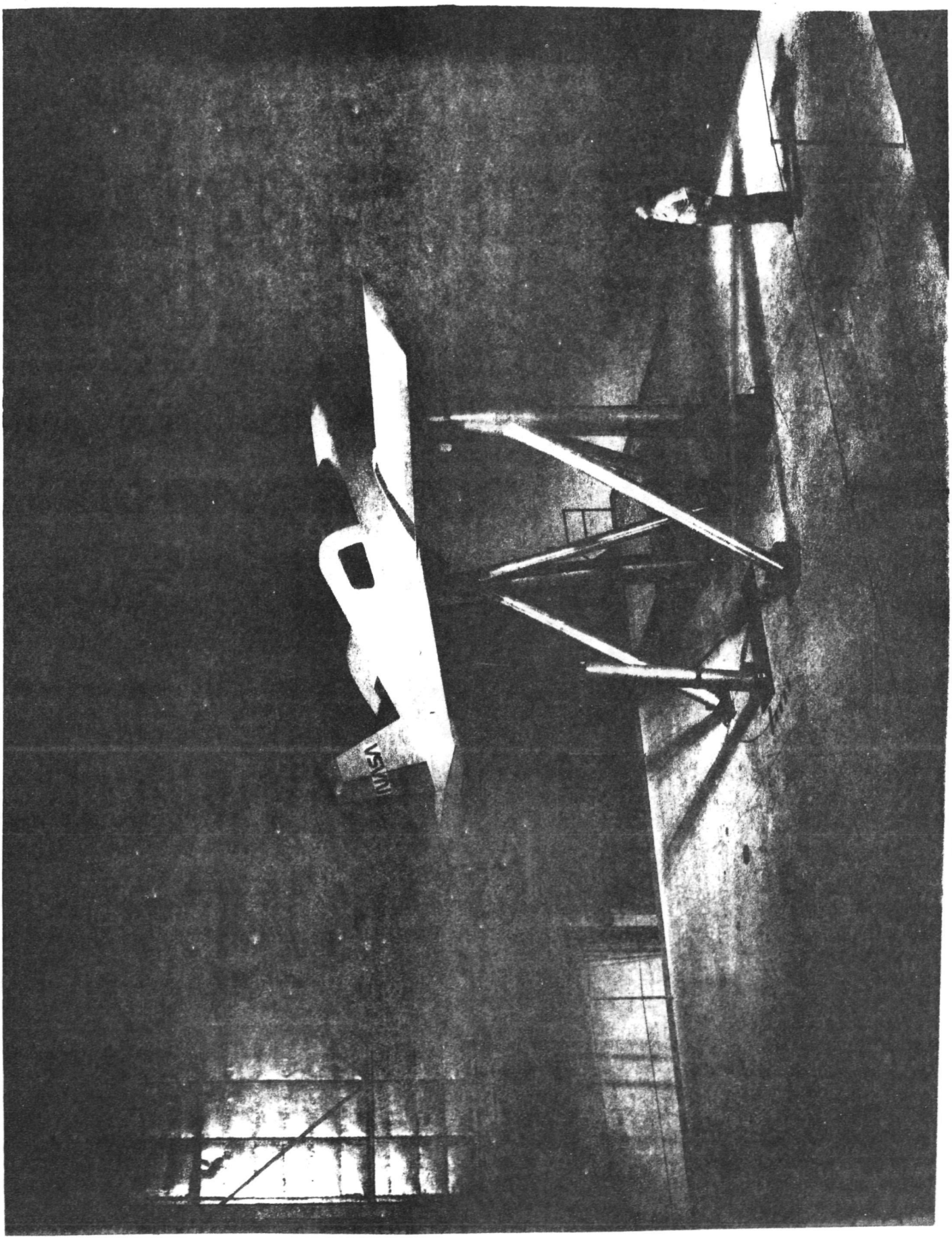

Figure 4. Photograph of Full Scale Model Installed in Tunnel

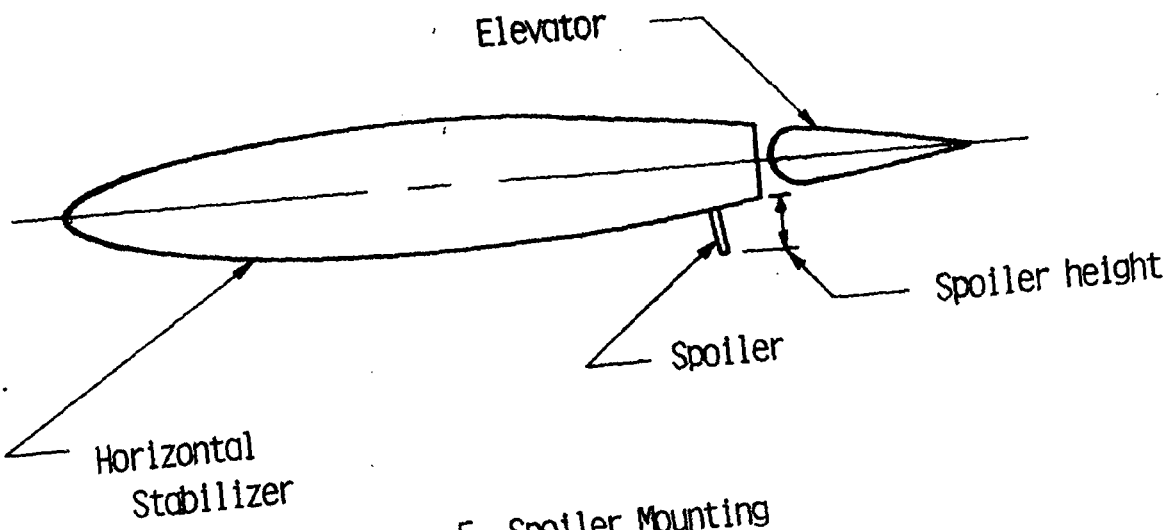

Figure 5. Spoiler Mounting

Test Conditions

The test section velocity was approximately 86 feet per second, corresponding to a test Reynolds number of 2.20×10^6. Table 1 lists aircraft geometry constants. Table 2 summarizes the airplane configurations and test conditions.

Table 1

Aircraft Geometry Constants

Wing Area, S_W	98.0 sq. ft.
Wing Span, b_w	24.46 ft
Wing Chord, c_W	4.00 ft
Tail Area, S_t	16.74 sq. ft.
Span of the Tail, b_t	7.690 ft
Elevator Area, S_e	7.22 sq. ft.
Elevator mean chord, $\bar{c}_e$	.95 ft
Tail length, l_t	11.620 ft.
Tail height, h_t	1.010 ft.

Table 2

Aircraft Test Configurations

α = 0 - 18 degrees, Flaps up

bhp	V_∞, fps	δ_e	h/c
0	86	0	0-.056
		-15	
		-23	
	94	0	
		-5	
		-10	
		-15	
13	86	0	0-0.064
		-5	
		-15	
		-20	
		-23	

α = 0 - 18 degrees, 30° Flaps

bhp	V_∞, fps	δ_e	h/c
18	86	0	0-.056
		-15	
		-23	
77	94	0	
		-15	
		-23	

Results

Stall Proofing the Test Aircraft

The first step in stall proofing an aircraft is to determine the usable angle of attack range. Figure 6 shows the test aircraft C_L variation with angle of attack for the power off, flaps up case. As shown, the usable angle of attack range extends to approximately 12 degrees. Beyond 12 degrees will be considered the stall regime. Although $C_{L_{max}}$ may be increased by changes in power and flap deflections, the change in stall angle of attack is negligible for this aircraft configuration. Figure 7 shows the additional case of power on and flaps deflected.

The onset of the stall has been labeled α_s in Figures 6 and 7. Previous studies[1,2,3,4] have shown that an angle of attack range of about 4° below stall is sufficient for the transition from basic to spoiler augmented stability. This was shown in Equation (2) and Figure 1. Therefore, with α_s = 12° and a 4° active range, spoiler deployment should begin at 8° angle of attack. This angle is labeled α_a.

Figure 8 shows the variation in pitching moment coefficient with changes in angle of attack for various elevator deflections. Although this is for the power off and flaps up case, the behavior of the curves around α_s is representative of all configurations and shows that the aircraft has no inherent pitch down (increase in the negative slope of the curve) at stall. Generally it is desirable to have a pitch down at stall to warn the pilot and aid in stall recovery efforts.

The small scale tests showed that, for a given angle of attack

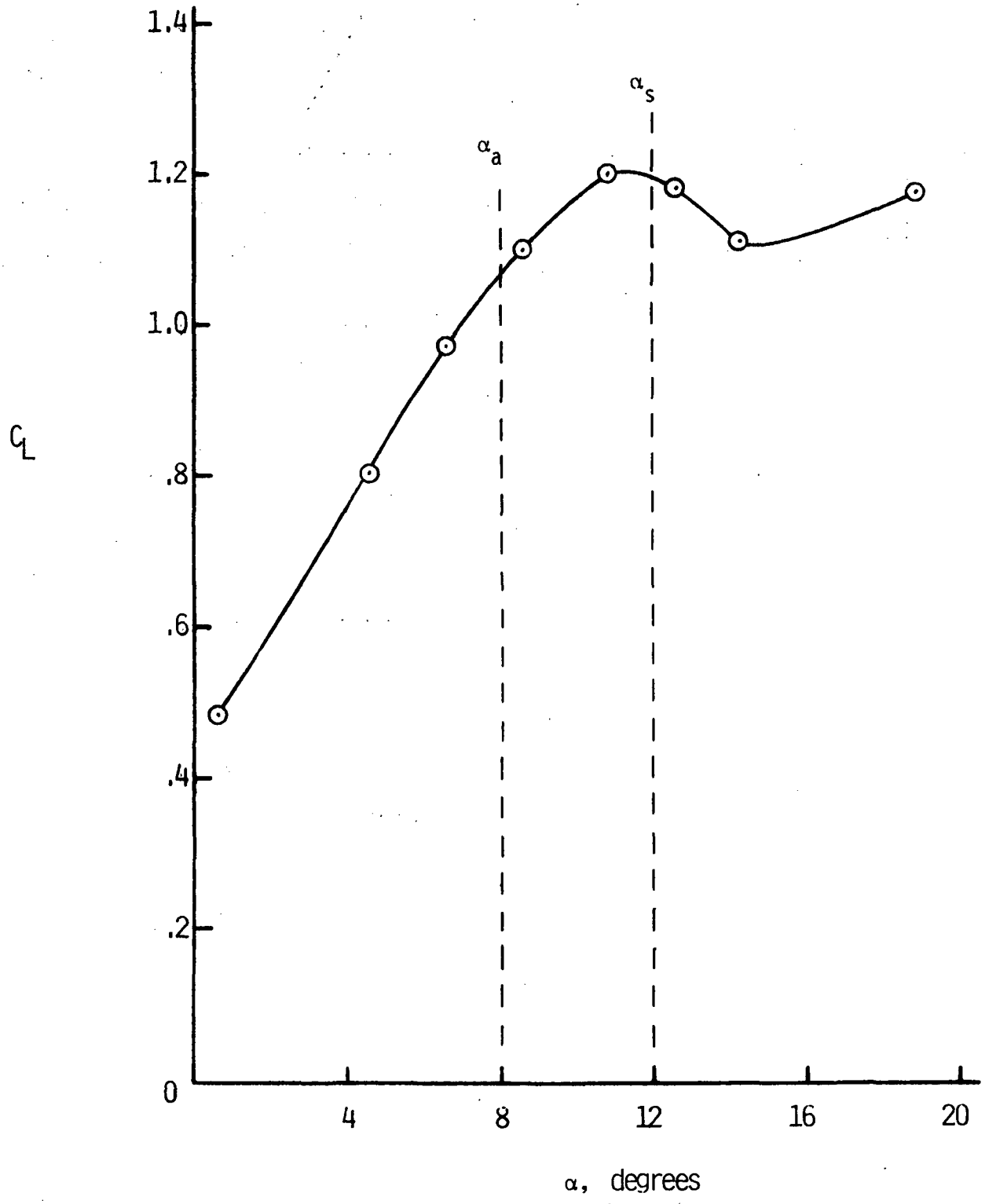

Figure 6. Variation of Lift Coefficient with Angle of Attack

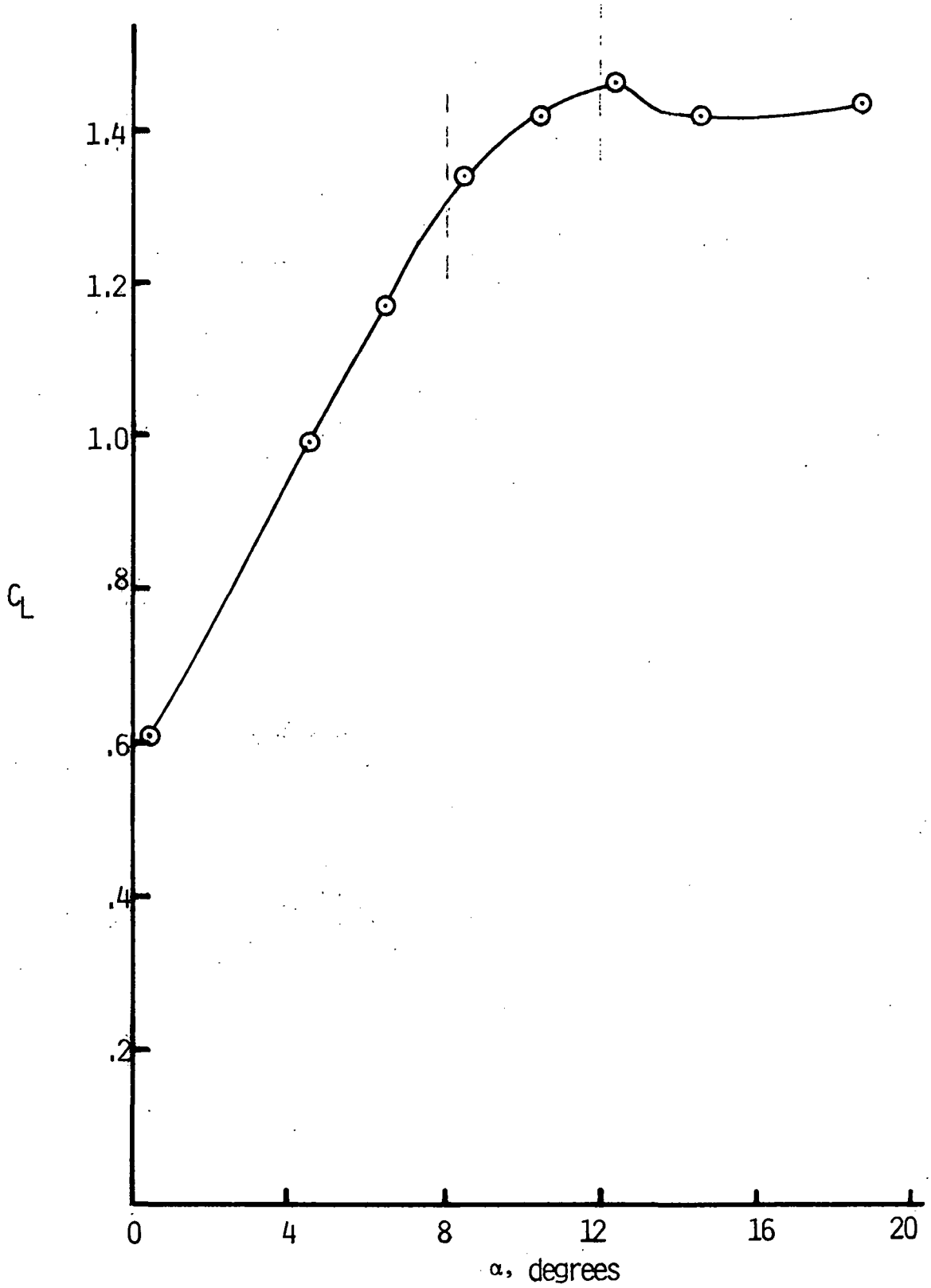

Figure 7. Variation of Lift Coefficient with Angle of Attack; 77 bhp, Flaps=30°

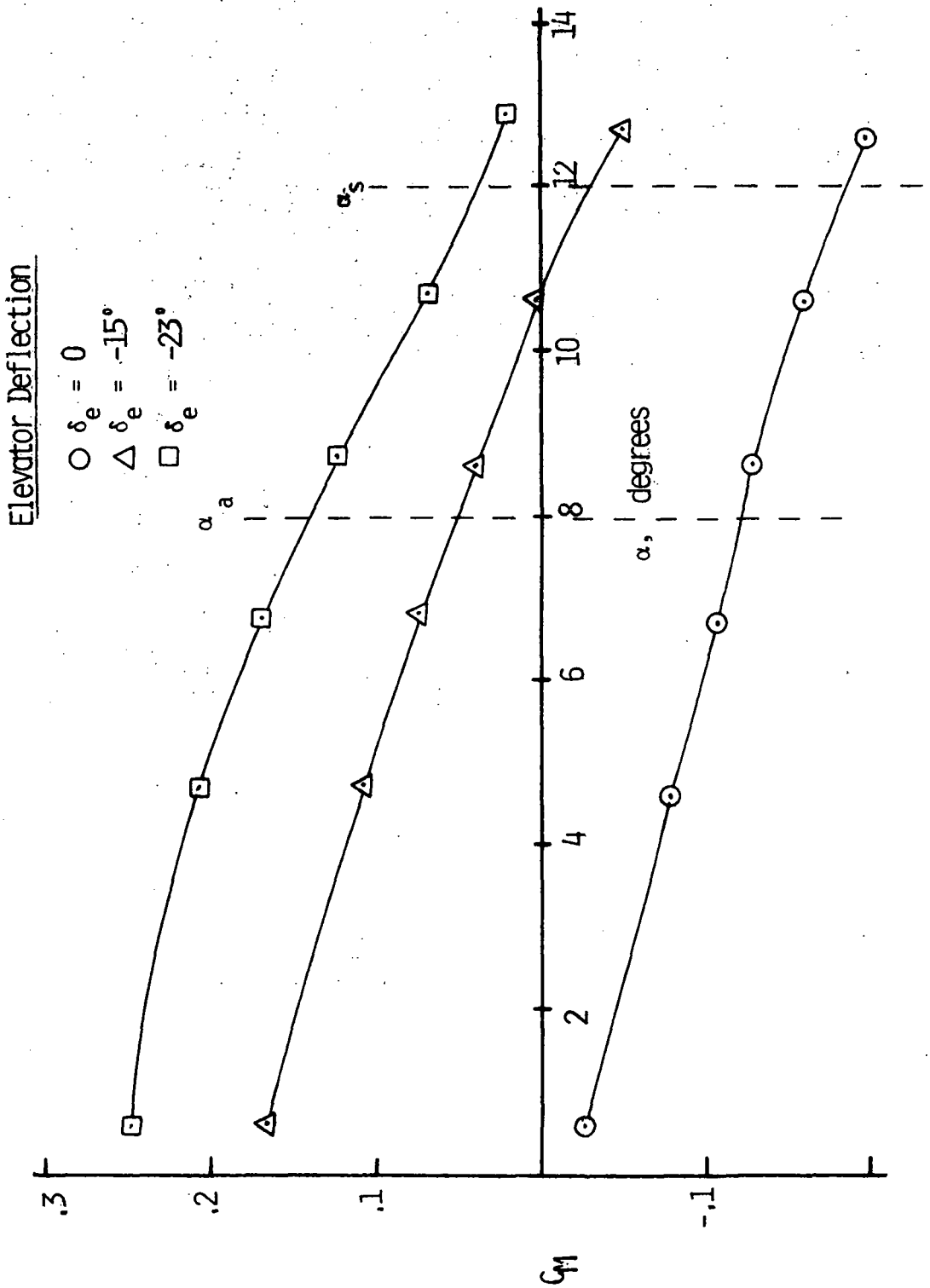

Figure 8. Variation of Pitching Moment Coefficient with Angle of Attack; Power off, No flaps

and elevator deflection, there was an almost linear reduction in pitching moment as spoiler height increased. Similar results were obtained for the full scale aircraft. Figure 9 shows this reduction in pitching moment up to a spoiler height of 0.056 for the test aircraft for $\alpha = 10°$ and power off. Similar results were obtained throughout the angle of attack range from 0 to 12° and for various power and flap configurations.

Using the full scale results shown in Figure 9 and the spoiler deployment program presented in Equation (2), the change in pitching moment coefficient for a programmed spoiler deployment can be obtained. Figure 10 shows this variation in pitching moment coefficient for the test aircraft. The curves below and the dashed lines above α_a represent the basic aircraft pitching moment coefficient and are identical to those in Figure 8. The solid lines represent the pitching moment coefficient due to the programmed spoiler deployment. The spoiler influenced pitching moment coefficient returns to the slope of the original curve beyond α_s; at which point the spoiler is fully deployed. The data in Figure 10 shows that the aircraft will trim below the stall angle of attack with full elevator deflection (-23°). There is also a sizable increase in static stability at the trim point. The slope of the curve, which is the static stability parameter, is much higher at the trim point, resulting in a much more stable airplane. This increase in stability fulfills the second fundamental requirement outlined in Reference 4; the aircraft should have a restoring moment at this trim condition which cannot be overcome by

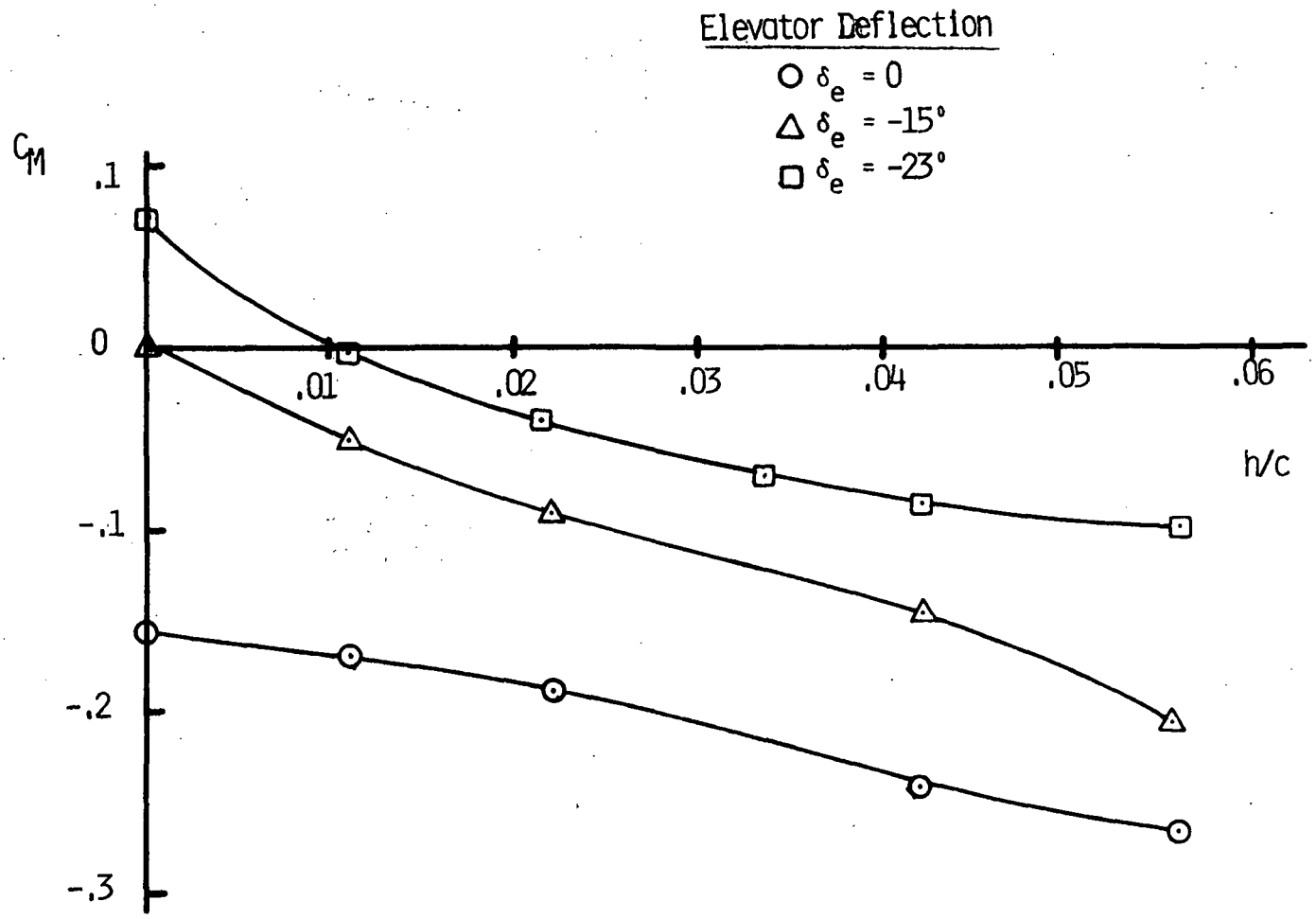

Figure 9. Variation of Pitching Moment Coefficient with Spoiler Height; Power off, No flaps, $\alpha = 10°$

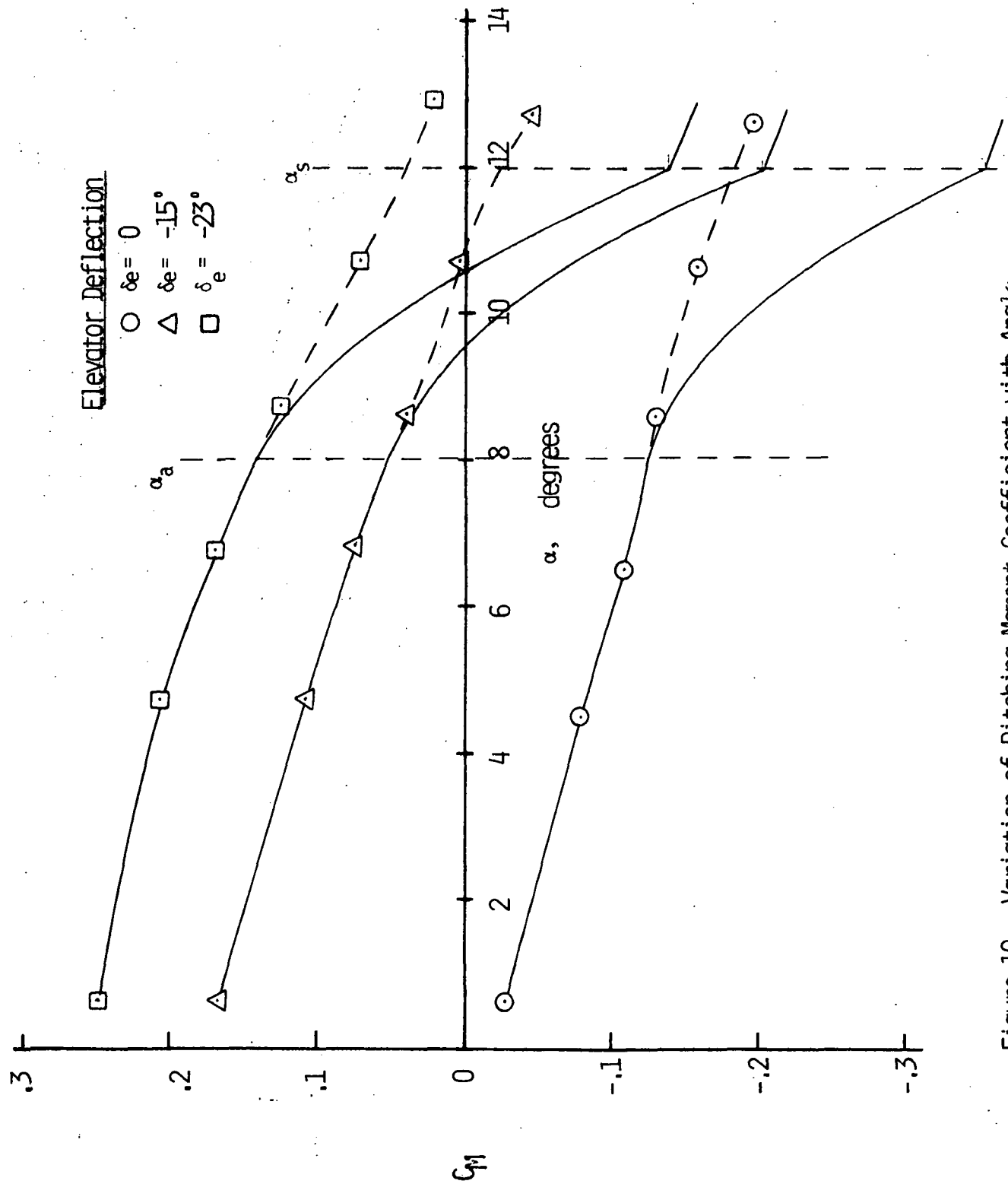

Figure 10. Variation of Pitching Moment Coefficient with Angle of Attack; Spoiler Augmented, Power off, No flaps

pilot or gust inputs. It must also be able to counteract any overshoot due to rotational inertia about the pitch axis. The slope of the pitching moment curve is a function of the spoiler deployment schedule which, thus far, has been based on intuition and previous experience[1,2]. More flight tests are needed to optimize this schedule.

It should be noted that the increased stability at high angles of attack should enhance both handling and safety by allowing the pilot to operate the airplane consistently and precisely near the stall angle of attack. The precise speed control which a highly stable aircraft is capable of would be a great aid during certain phases of flight such as takeoffs and landings or instrument approaches.

Figures 8, 9, and 10 represent the power off, flaps up case. Figures 11, 12, and 13 show data for power on, and full flap deflection. In terms of the spoiler's ability to prevent the aircraft from stalling, this was the most severe case tested. As seen by the wider spacing between the curves in Figure 11 as compared to Figure 8, elevator effectiveness has increased by about 40%. Comparison of Figure 12 with Figure 9 shows that for the same change in configuration, the spoiler effectiveness only increased about 23%. Figure 13 shows the same results as Figure 10 for the full flaps and power on case. Figures 10 and 13 illustrate two extremes in configurations for which the spoiler must stall proof the aircraft. For this range of configurations, the loss in maximum usable angle of attack is approximately 1.0°. Referring to Figure 6, this represents less than a 2% loss in the maximum available lift coefficient.

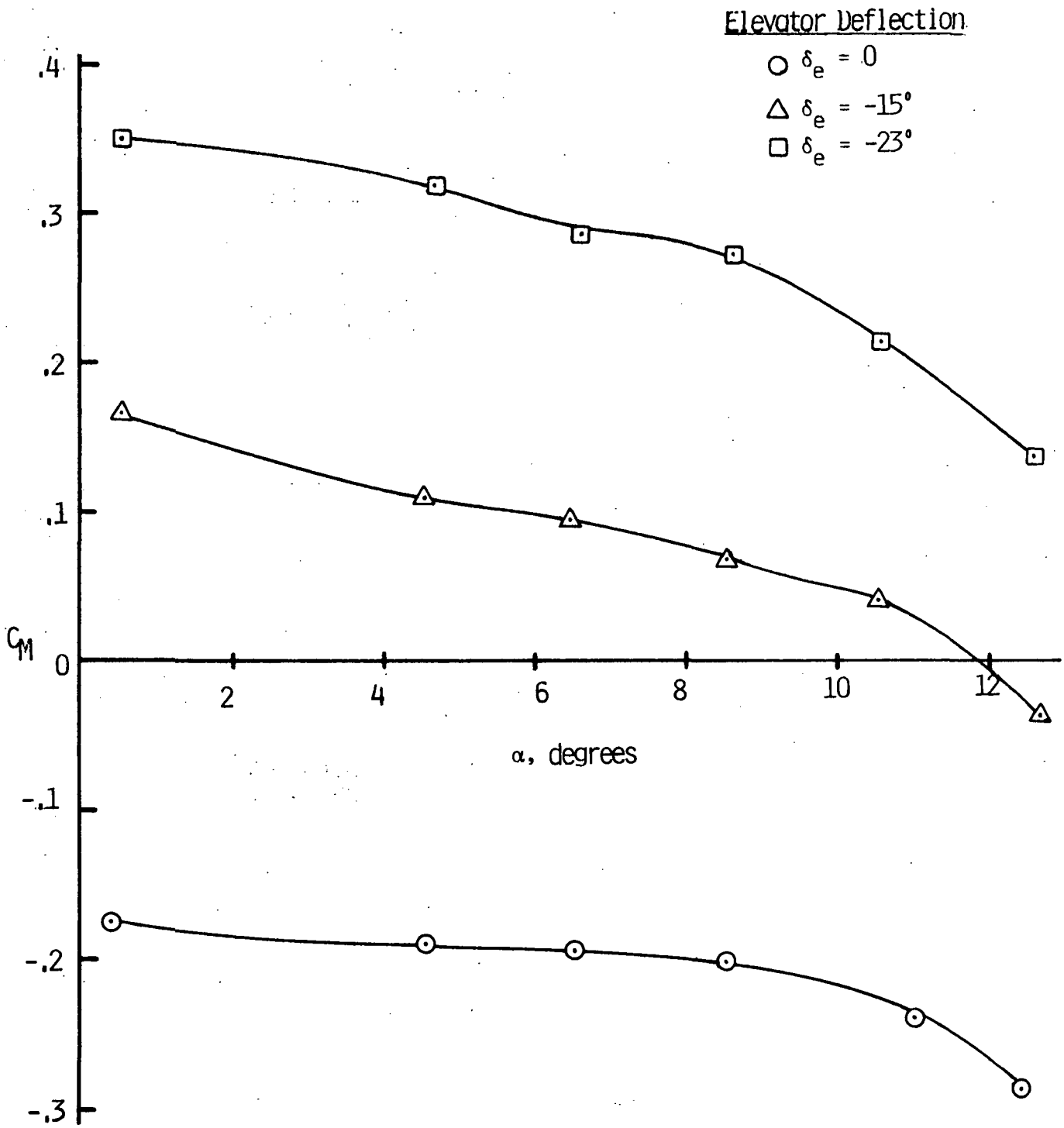

Figure 11. Variation of Pitching Moment Coefficient with Angle of Attack; Power on, Flaps=30° h/c = 0°

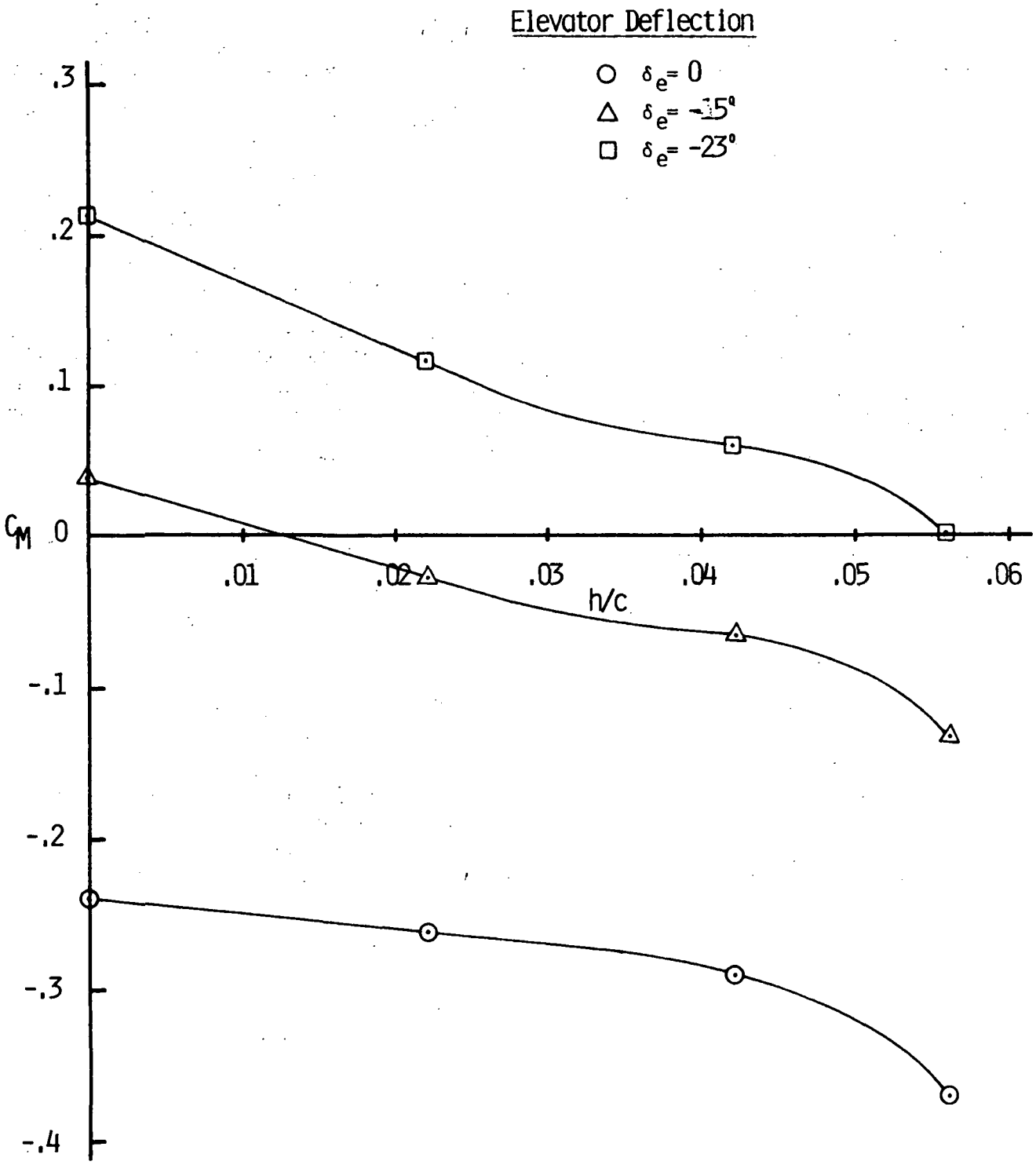

Figure 12. Variation of Pitching Moment Coefficient with Spoiler Height; 77 bhp, 30° Flaps, α = 10°

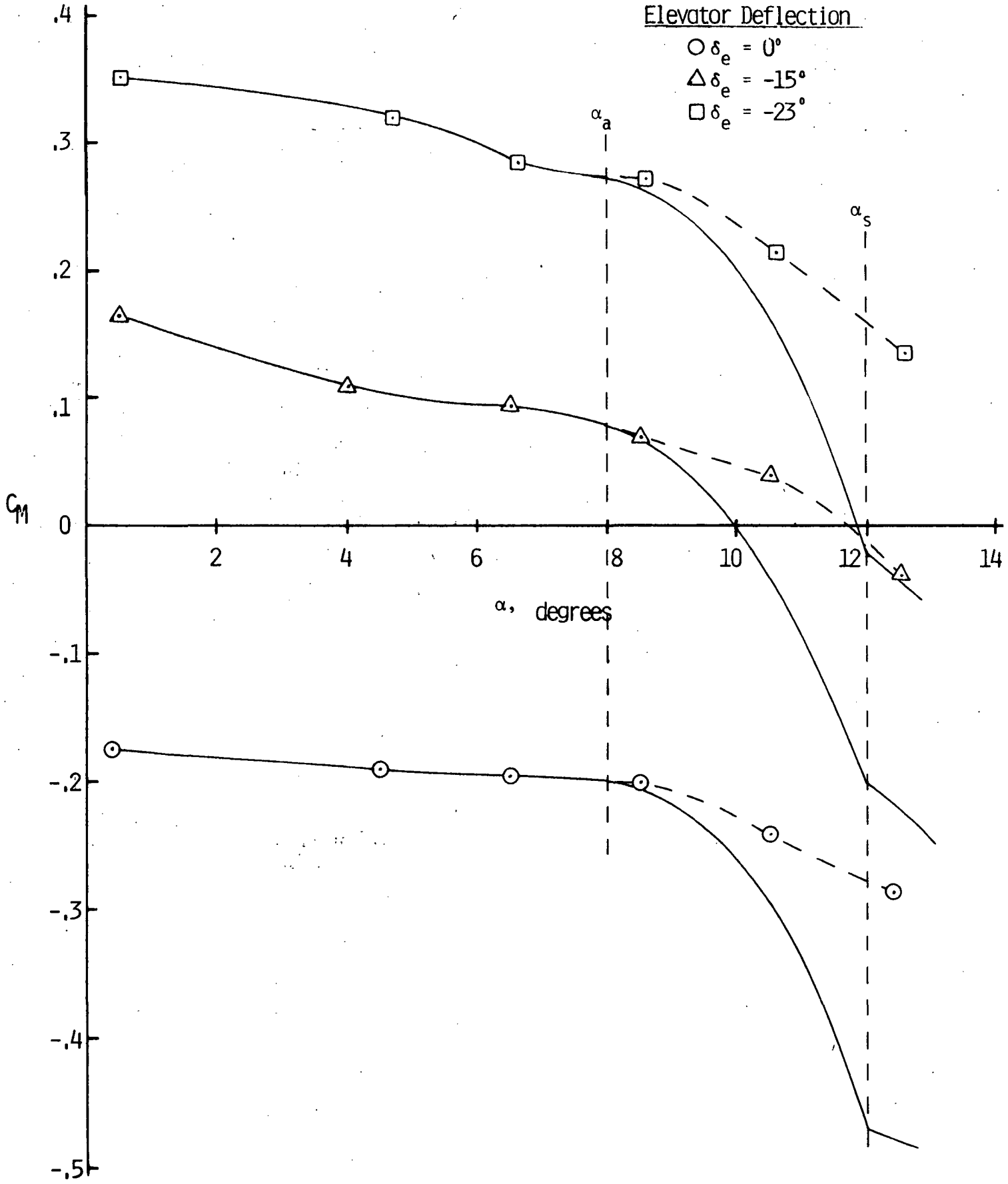

Figure 13. Variation of Pitching Moment Coefficient with Angle of Attack; Spoiler Augmented, 77 bhp, 30°

For the power on, full flap configuration, the aircraft is trimmed much closer to the stall angle of attack. The 77 bhp condition is not the maximum power available and with an increase in power, a slightly larger spoiler height may be required for complete stall proofing.

All data presented have been corrected to a c.g. location of 25% chord. This reflects a trim condition ($\delta_e = 0$) of $\alpha = 1.0°$, corresponding to a C_L of approximately 0.35. The effects of moving the c.g. forward would be to change the trim condition and increase the static stability of the aircraft. Both would enhance the spoiler's effectiveness as a stall preventative system.

Correlation of Results with Previous Tests

The primary purpose of the full scale tests was to verify the results and conclusions obtained from the theoretical approach and previous wind tunnel tests.

Probably one of the more difficult problems in designing the spoiler deployment system is determining the increase in stability which must be provided by the spoiler and the maximum usable angle of attack. The solution is severely affected by changes in Reynolds number. The problem is illustrated in Figure 14, which shows the variation in lift coefficient with angle of attack for two Reynolds numbers. The curve for $R_N = 2.97 \times 10.5$ represents data for the 1/5 scale model tested in the 12 foot low speed wind tunnel. As noted,

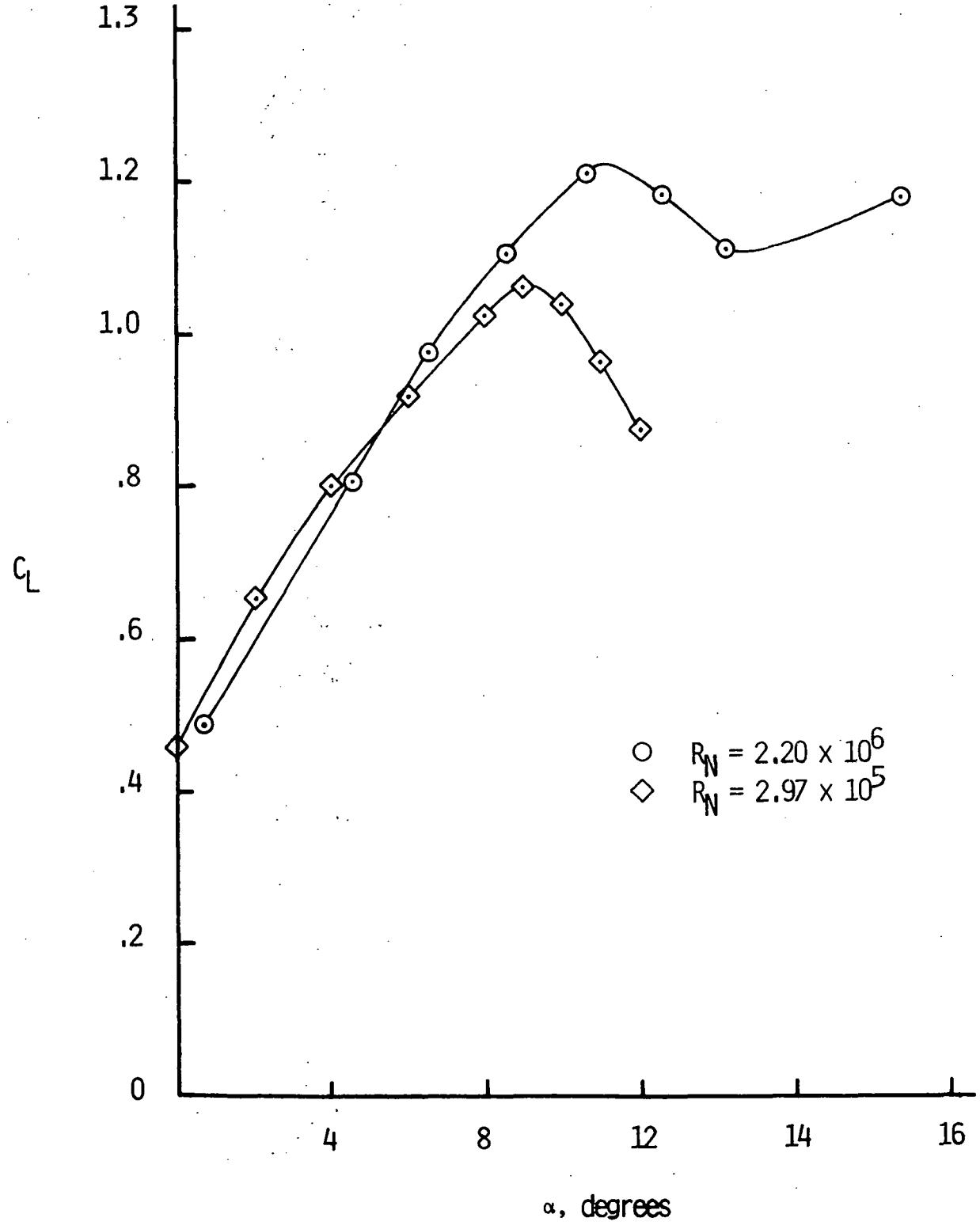

Figure 14. Reynolds Number Effects on Lift Coefficient

flow separation and the resulting stall occurred at approximately 9° angle of attack whereas for the full scale tests, stall did not begin until approximately 12°. In addition, the break in the lift curve was more severe for the small scale tests. It is evident from this comparison that low Reynolds number tests are not suitable for determining stall onset or the usable angle of attack range for the full scale airplane. This would have to be determined from flight tests or high (equal to full scale flight R_N) Reynolds number wind tunnel tests.

Figure 15 compares the variation in pitching moment coefficient with angle of attack for the same tests. The curves do not coincide at low angles of attack due to differences between the horizontal tail incidence angles; however, the slopes of the two curves are very similar up to the point where the stall begins on the low R_N test. Beyond the stall, the low R_N test demonstrates a marked increase in the slope of the pitching moment curve not evident in the high R_N test. Since the spoiler will be designed to operate in a region below the stall angle of attack, for preliminary design purposes, the small scale tests would provide adequate data regarding pitching moment in this regime.

Reference 5 describes the testing of the horizontal tail only of the test aircraft in the Texas A&M 7 x 10 foot low speed wind tunnel. The test fulfilled three basic requirements: (1) To verify some of the results of the small scale tests[4], (2) To verify the theoretical approach developed in References 3 and 4, and (3) to optimize spoiler

flow separation and the resulting stall occurred at approximately 9° angle of attack whereas for the full scale tests, stall did not begin until approximately 12°. In addition, the break in the lift curve was more severe for the small scale tests. It is evident from this comparison that low Reynolds number tests are not suitable for determining stall onset or the usable angle of attack range for the full scale airplane. This would have to be determined from flight tests or high (equal to full scale flight R_N) Reynolds number wind tunnel tests.

Reference 5 describes the testing of the horizontal tail only of the test aircraft in the Texas A&M 7 x 10 foot low speed wind tunnel. The test fulfilled three basic requirements: (1) to verify some of the results of the small scale tests[4], (2) to verify the theoretical approach developed in References 3 and 4, and (3) to optimize spoiler configuration and location. The geometry of the spoiler for the full scale test was based on the tail only tests.

Since a change in aircraft pitching moment can be viewed as a change in tail lift, it was hoped that the results of the tail only test could also be used to predict the response of the full scale aircraft to spoiler and elevator deflections. Analysis of the full scale data shows that trends can be predicted but the prediction of absolute values requires accurate knowledge of the flow field characteristics in which the tail is operating. For example, problems were encountered in trying to compute a tail efficiency factor, η_T. This was done by comparing the pitching moment derivatives of the full scale aircraft with and without the tail attached. Figure 15 shows the

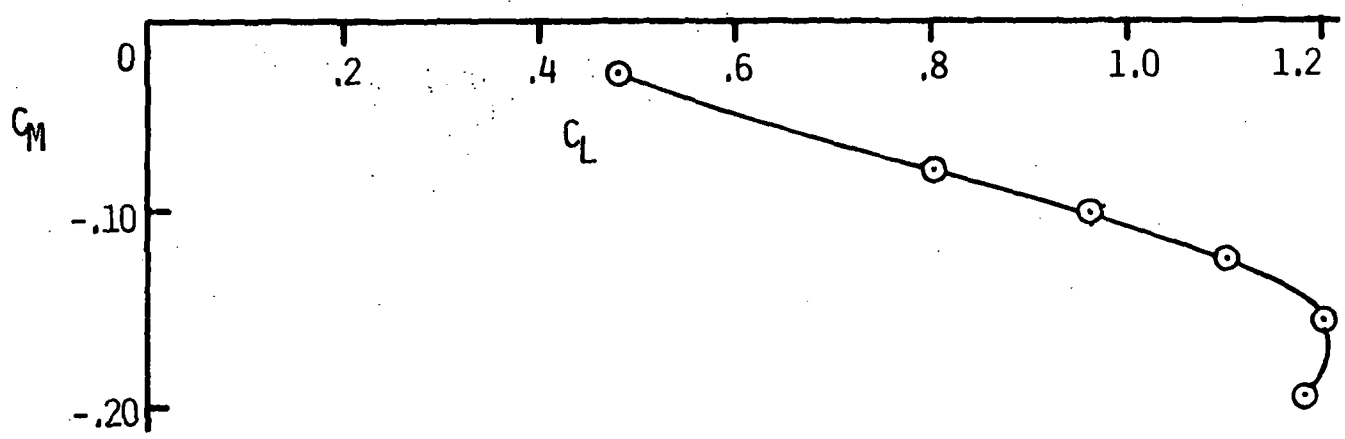

Figure 15. Variation of Pitching Moment Coefficient with Lift Coefficient; Complete Airplane

pitching moment variation with changes in lift coefficient for the complete configuration. The slope of the curve, $\frac{d_{CM}}{d_{CL}}$, is essentially constant in the region below stall with a value of -.1519. Figure 16 shows the same curve for the airplane without the tail. If this curve is linearized as shown by the dashed line, the resulting slope is .0700. From the static stability equations of Reference 6, the change in the pitching moment coefficient of the aircraft with changes in lift coefficient can be summarized as follows:

$$\left(\frac{dC_M}{dC_L}\right)_{aircraft} = \begin{pmatrix}\text{Contribution due to}\\ \text{the wing, fuselage}\\ \text{and misc. components}\end{pmatrix} + \begin{pmatrix}\text{Contribution}\\ \text{due to the tail}\end{pmatrix}$$

The contribution due to the tail can be further broken down as follows:

$$\left(\frac{dC_M}{dC_L}\right)_{tail} = \frac{m_T}{m_W}\ \bar{V}\,\eta_T\left(1 - \frac{d\varepsilon}{d\alpha}\right) \qquad (3)$$

The lift curve slope of the wing-body can be determined from Figure 17 while Figure 18 from Reference 5, provides the same data for the tail alone. The slopes are .0746 and .0495 for the wing-body and tail alone respectively. The value of $\frac{d\varepsilon}{d\alpha}$, .414, was estimated using NACA TR 648[7]. Since $\left(\frac{dC_M}{dC_L}\right)_{tail}$ can be determined by subtracting the wing-body contribution from the $\left(\frac{dC_M}{dC_L}\right)_{aircraft}$, the tail efficiency factor, η_T, is the only unknown

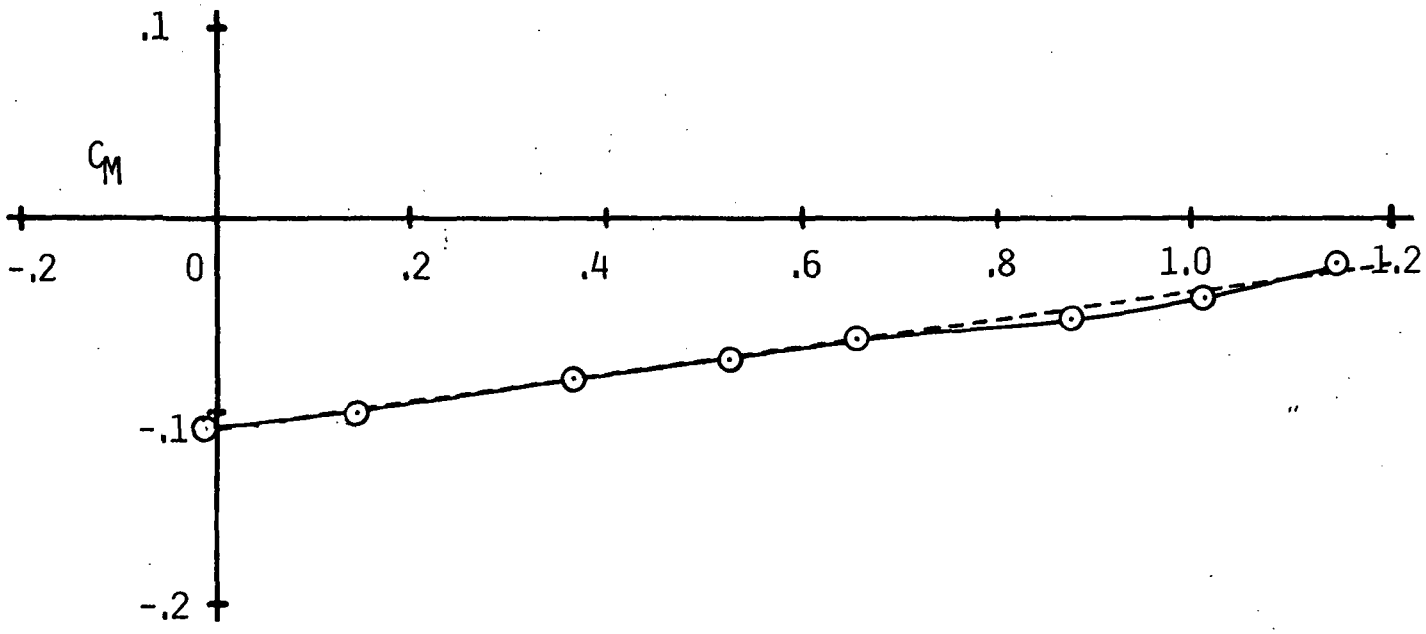

Figure 16. Variation of Pitching Moment Coefficient with Lift Coefficient; Wing-Body

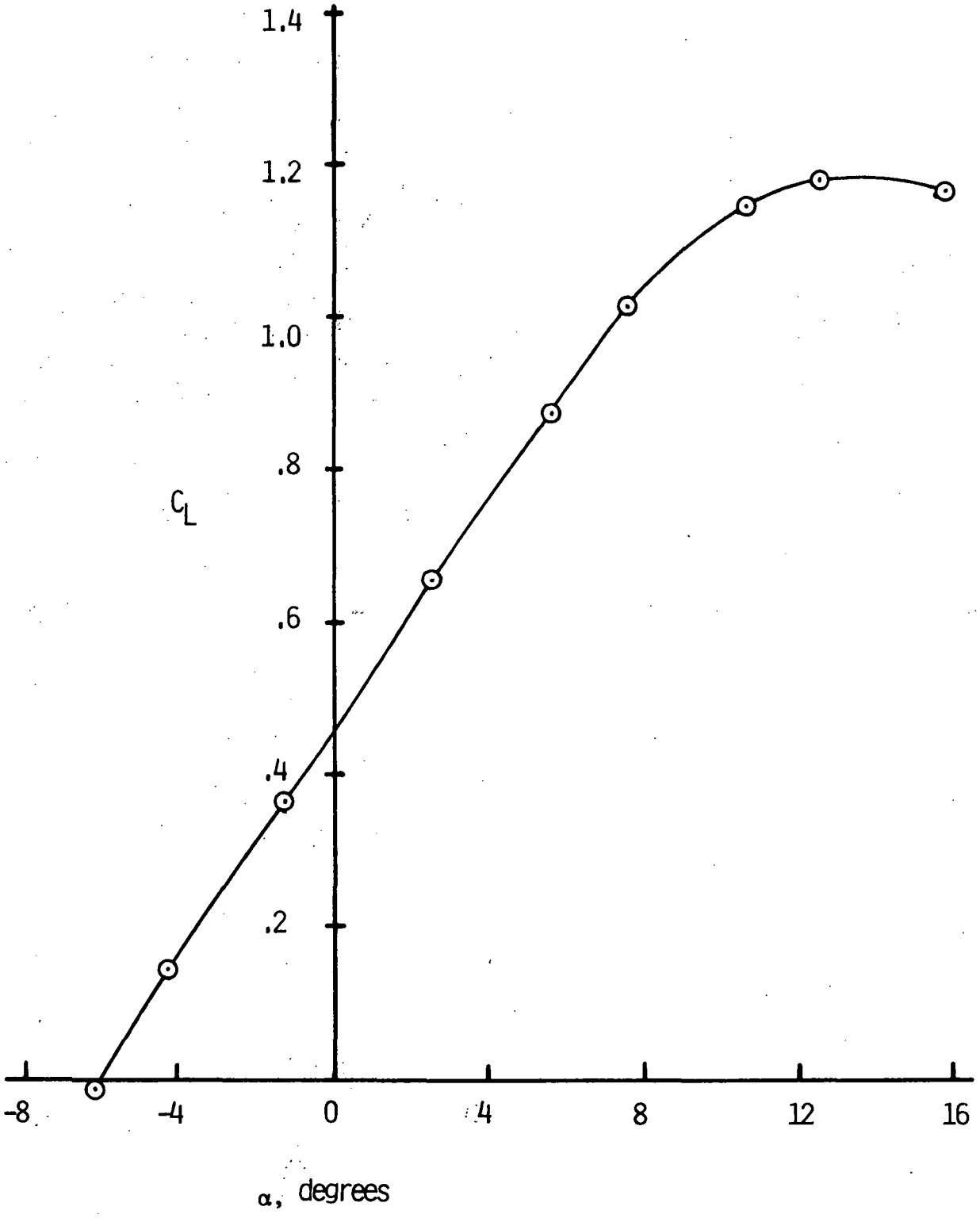

Figure 17. Variation of Lift Coefficient with Angle of Attack; Power off, Wing-Body

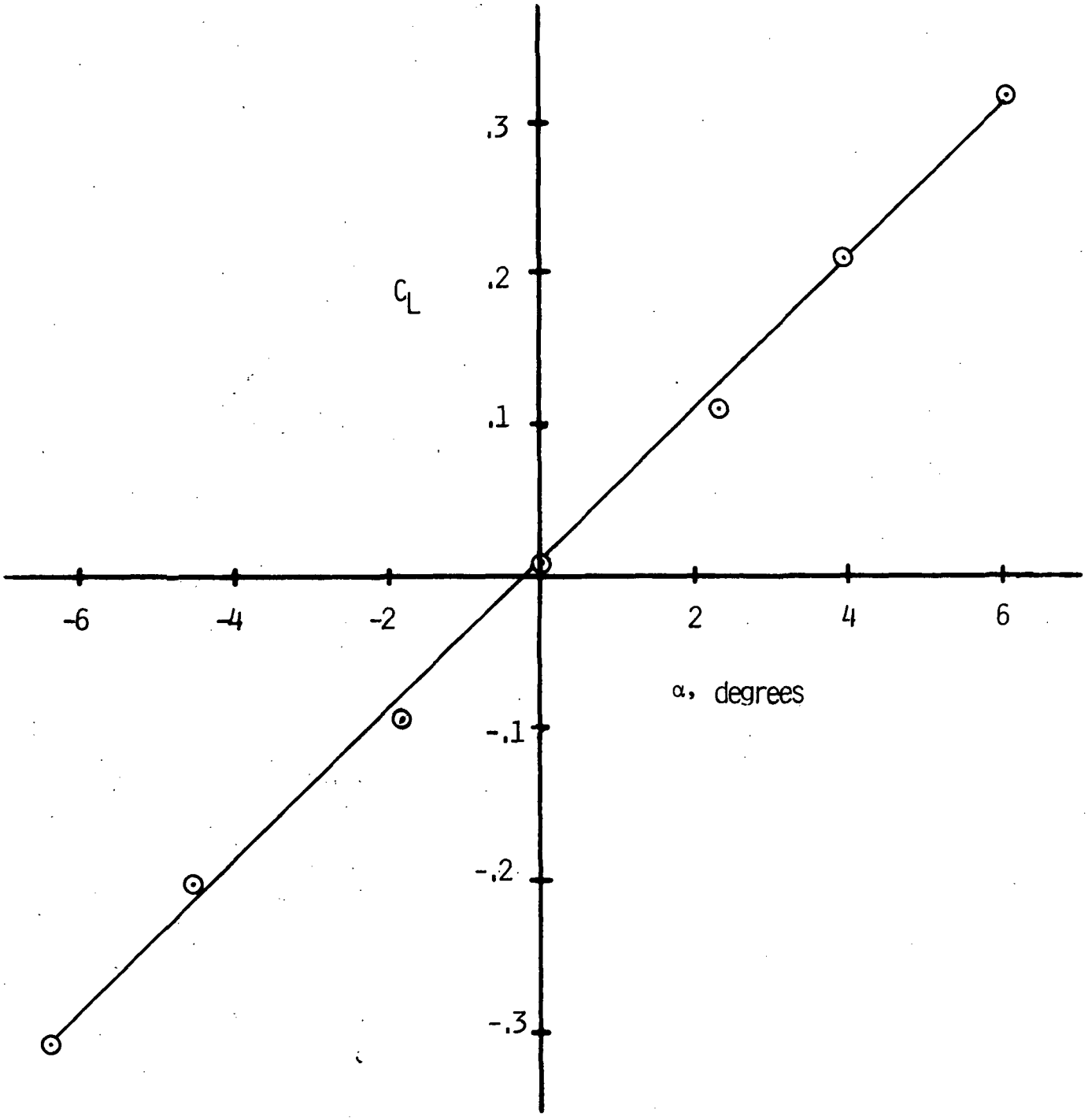

Figure 18. Variation of Lift Coefficient with Angle of Attack; Tail only

in equation (3);

$$\eta_T = - \frac{\left(\frac{dC_M}{dC_L}\right)_{aircraft} - \left(\frac{dC_M}{dC_L}\right)_{wing\text{-}body}}{\left(\frac{m_T}{m_W}\right)\left(\frac{S_T}{S_W}\right)\left(\frac{\ell_T}{c}\right)\left(1 - \frac{d\epsilon}{d\alpha}\right)} \qquad (4)$$

$$= 1.15$$

An efficiency factor of 115% is unrealistic. Since the values for all variables in Equation (3) except $\frac{d\epsilon}{d\alpha}$ were obtained experimentally, it must be assumed that the actual value of $\frac{d\epsilon}{d\alpha}$ is significantly smaller than that derived from Reference 7. Thus, prediction of actual values of full scale pitching moments using the data from Reference 5 could not be accomplished without knowledge of the actual downwash characteristics. As shown in Equations (5) and (6), the variable $\frac{d\epsilon}{d\alpha}$ does not appear in the elevator or spoiler stability derivatives, so they may be predicted reasonably well using data obtained from the tail alone tests and an assumed η_T of 1.0.

$$\frac{\partial C_M}{\partial \delta_e} = \bar{V} \eta_T \frac{\partial C_{L_T}}{\partial \delta_e} \qquad (5)$$

$$\frac{\partial C_M}{\partial h/c} = \bar{V} \eta_T \frac{\partial C_{L_T}}{\partial h/c} \qquad (6)$$

In Figure 19, changes in the full scale pitching moment coefficient with elevator deflection are compared with a curve which was "predicted" using the data from Reference 5. The slope of the predicted curve was calculated using Equation (5). However, the starting point (δ_e=0) had to be calculated using the downwash characteristics obtained from

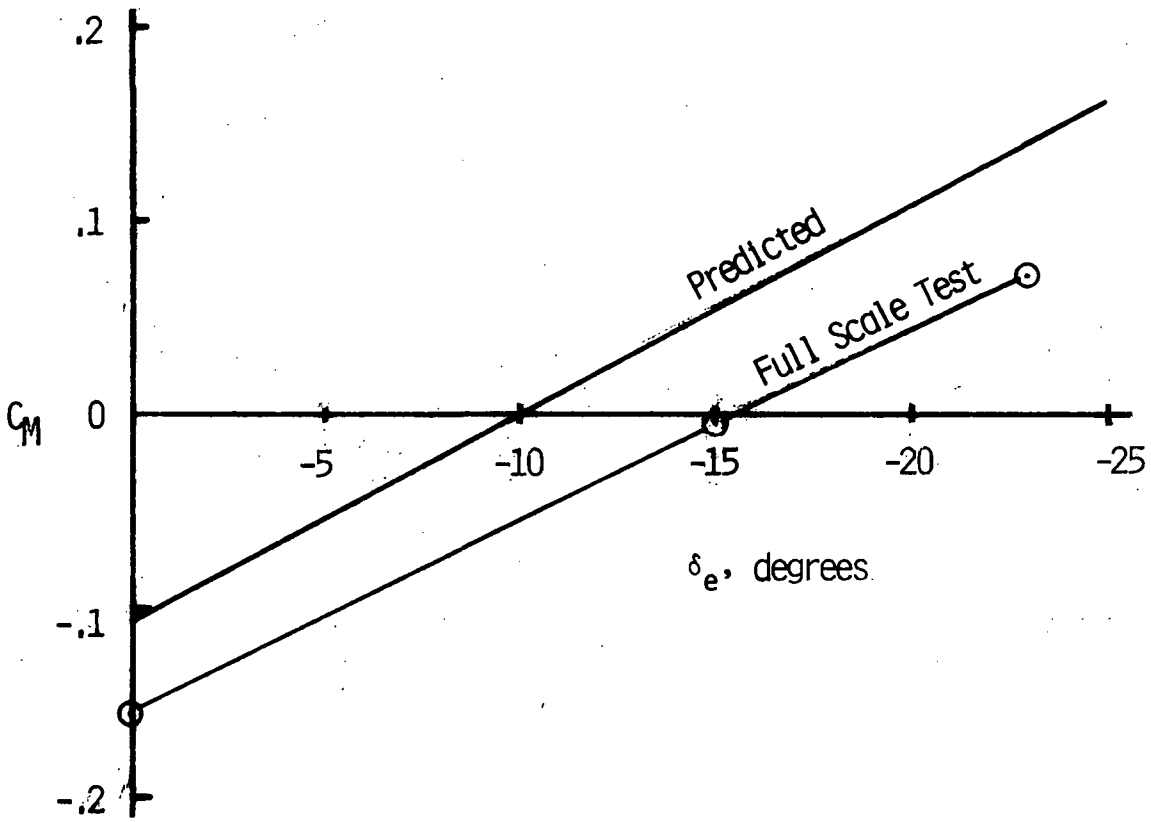

Figure 19. Variation of Pitching Moment Coefficient with Elevator Deflection

Reference 7 and a theoretical wing lift curve slope of 4.71 instead of the actual 4.27. Thus, while the absolute value of the aircraft pitching moment for a given elevator deflection cannot be accurately predicted, the derivative can. Figure 20 shows a similar comparison for pitching moment coefficient as a function of spoiler height.

A comparison of full scale airplane and tail only data for elevator hinge moment coefficient is shown in Figure 21. This is for elevator hinge moment coefficient as a function of spoiler height but is typical of the poor correlation between the two tests for all hinge moment data. One reason for the poor correlation could be differences in the flow field; the tail only was operating in a free airstream whereas the tail on the aircraft was operating in the wake of the wing and fuselage. Another possibility could be differences in spoiler attachment. Note the large change in C_{h_e} for a change from 0 to .01 h/c for the tail only test. This indicates that C_{h_e} is very sensitive to small perturbations on the lower surface of the horizontal stabilizer. A value of .01 h/c corresponds to approximately .31 inches. For the tail alone tests, h/c = 0 corresponded to a clean lower surface. However, for the full scale tests, even in the fully retracted position (h/c = 0), the spoiler provided a discontinuity on the lower surface. This amounted to approximately .10 inch and was necessary since the entire spoiler and hinge assembly was mounted externally. It is not possible to identify a specific cause for the differences between the tests at this time.

Both tests do, however, show an increase in hinge moment as the spoiler is deployed. It should be understood that while some of the increase in stick force identified in Reference 4 will be directly due to spoiler deployment, most will be due to the increase in stability provided by the spoiler.

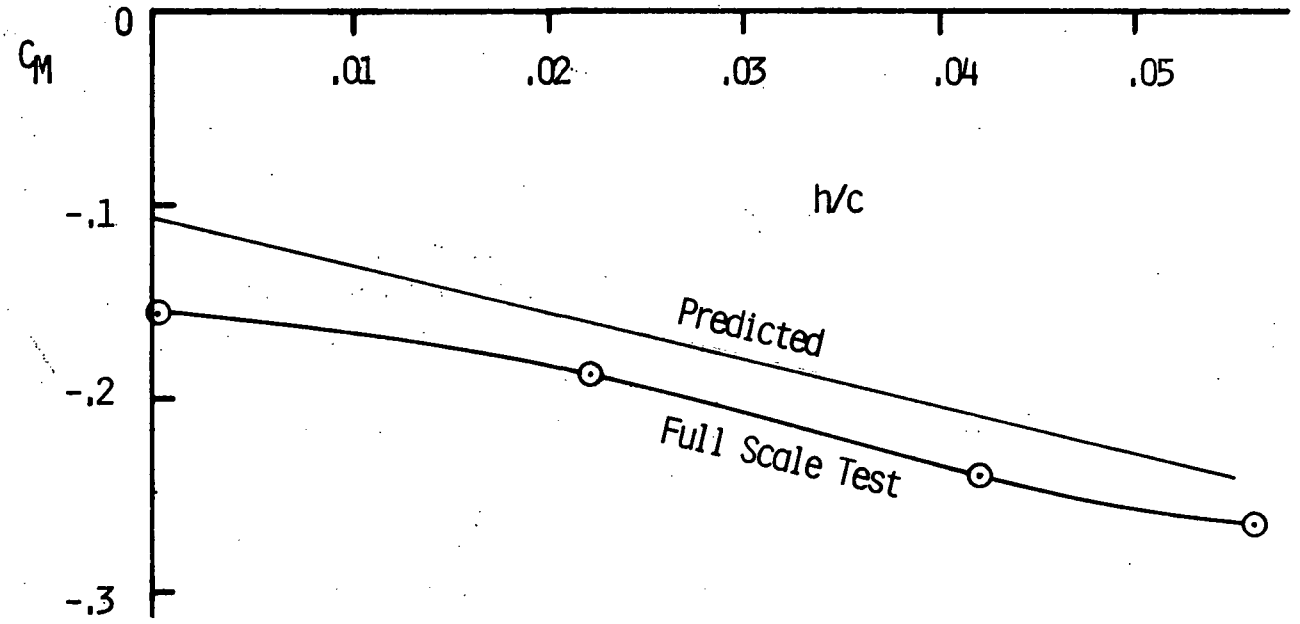

Figure 20. Variation of Pitching Moment Coefficient with Spoiler Height; $\delta_e=0°$, $\alpha=10°$

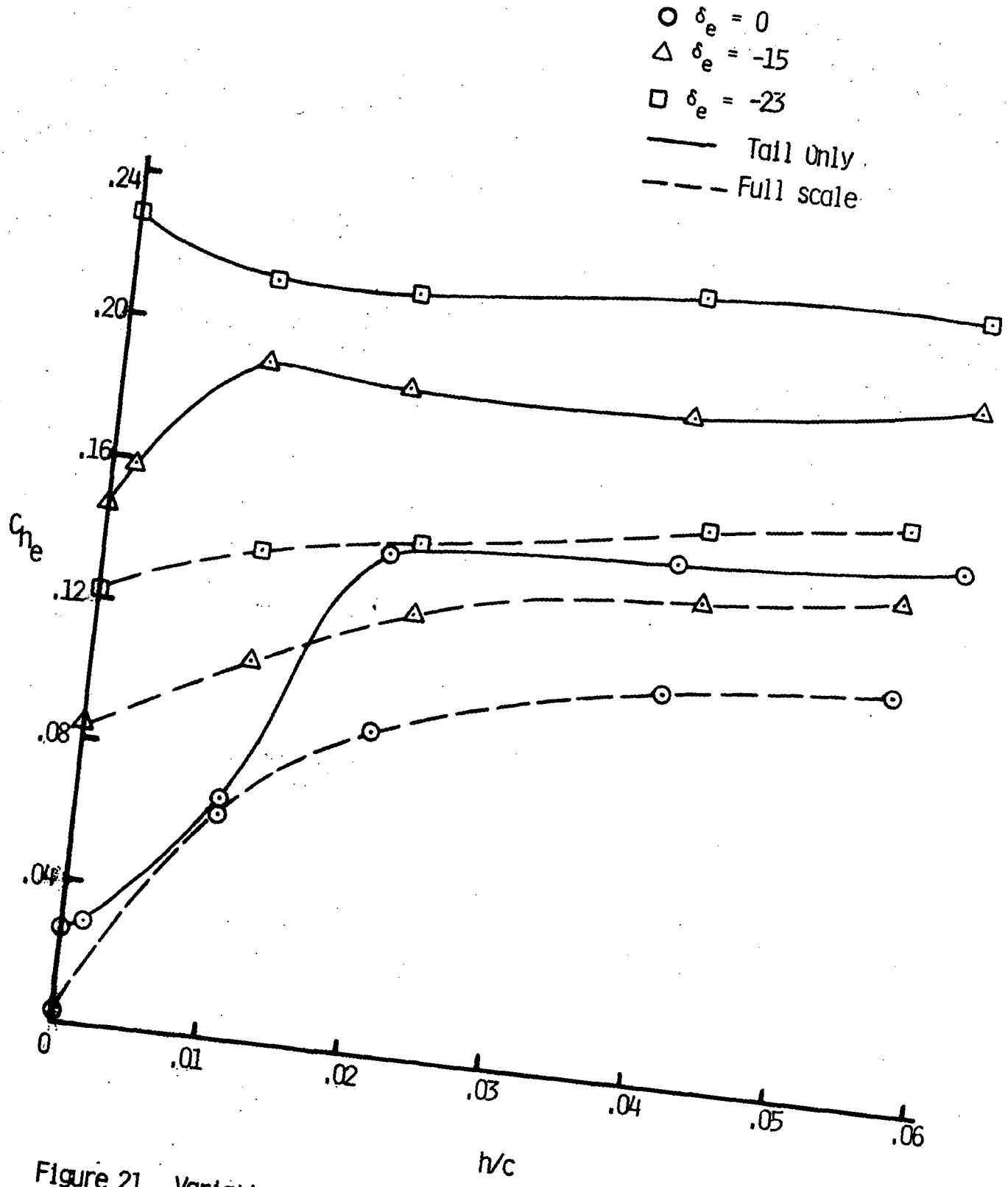

Figure 21. Variation of Elevator Hinge Moment Coefficient with Spoiler Height; $\alpha_{fuselage}=10°$, $\alpha_{tail}=4°$

Effects of Spoiler and Elevator Deflection

Figure 22 depicts the aircraft pitching moment as a function of elevator deflection for $\alpha = 10°$ and no power. The top curve represents no spoiler deflection while the bottom curve is for $h/c = 0.056$, which was the maximum height tested.

While the slope, $C_{M_{\delta_e}}$, remains essentially linear throughout the spoiler deployment, there is a slight reduction in its slope at full deployment. This indicates that the deployment of the spoiler has not changed the characteristics of the elevator. For this aircraft, elevator effectiveness, $C_{M_{\delta_e}}$, increased significantly with increases in power and flap deflection; however, the effect of spoiler deployment on elevator power remained small regardless of configuration changes. This is illustrated in Figure 23, where the slope of the curve of the variation in pitching moment with changes in elevator deflection angle has increased considerably due to increases in power and flap deflection but the change in $C_{M_{\delta_e}}$ due to spoiler deployment has remained small.

Figure 24 shows the variation in pitching moment coefficient with changes in spoiler height. There is a tendency for the spoiler to gain effectiveness ($\partial C_M / \partial h/c$) as the elevator is deflected. This is noticeable only for the high power, large flap deflection case shown in Figure 25. The effect become undetectable with power off and no

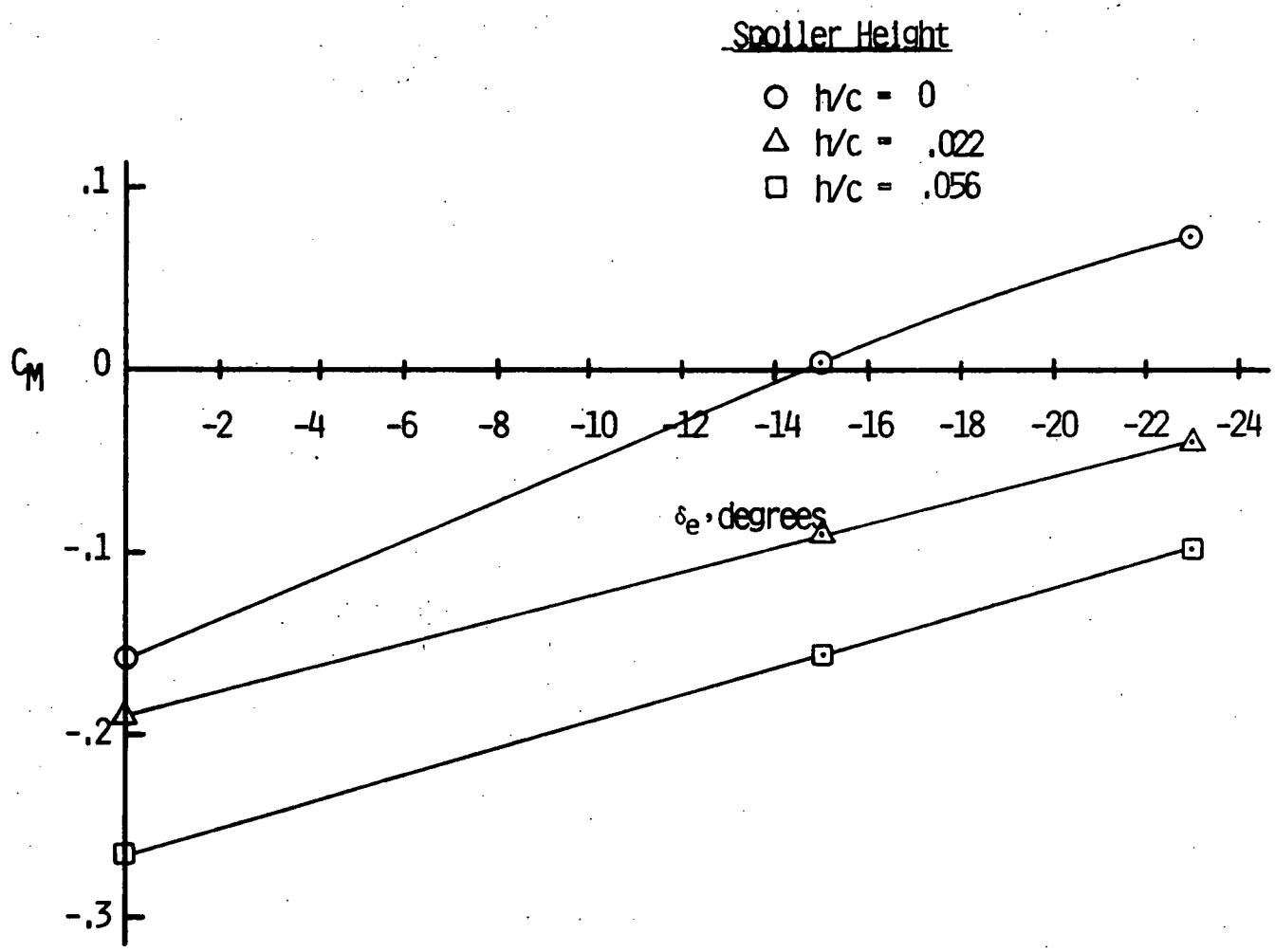

Figure 22. Variation of Pitching Moment Coefficient with Elevator Deflection; No power, No flaps, α=10°

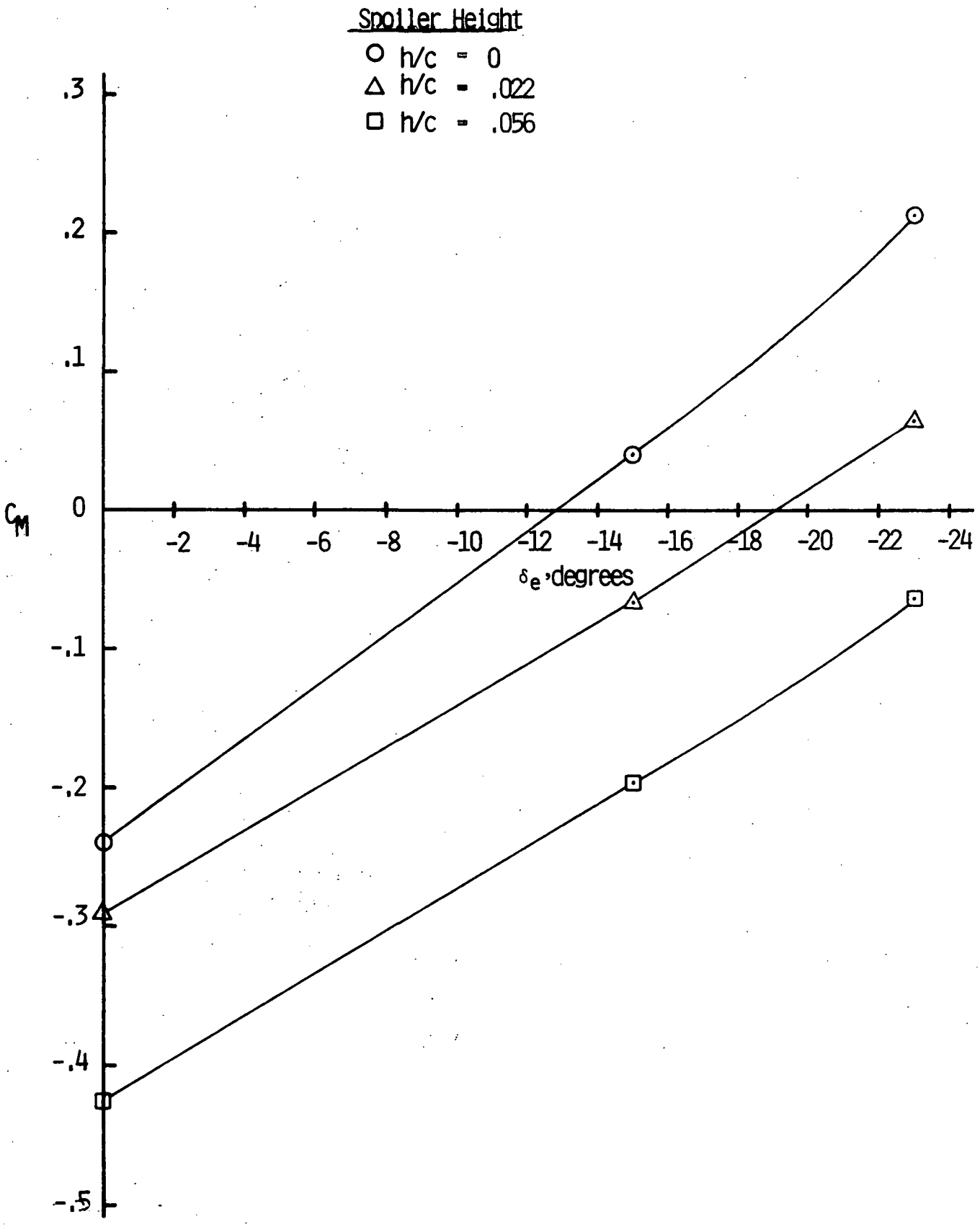

Figure 23. Variation of Pitching Moment Coefficient with Elevator Deflection; 77 bhp, 30° Flaps, $\alpha = 10°$

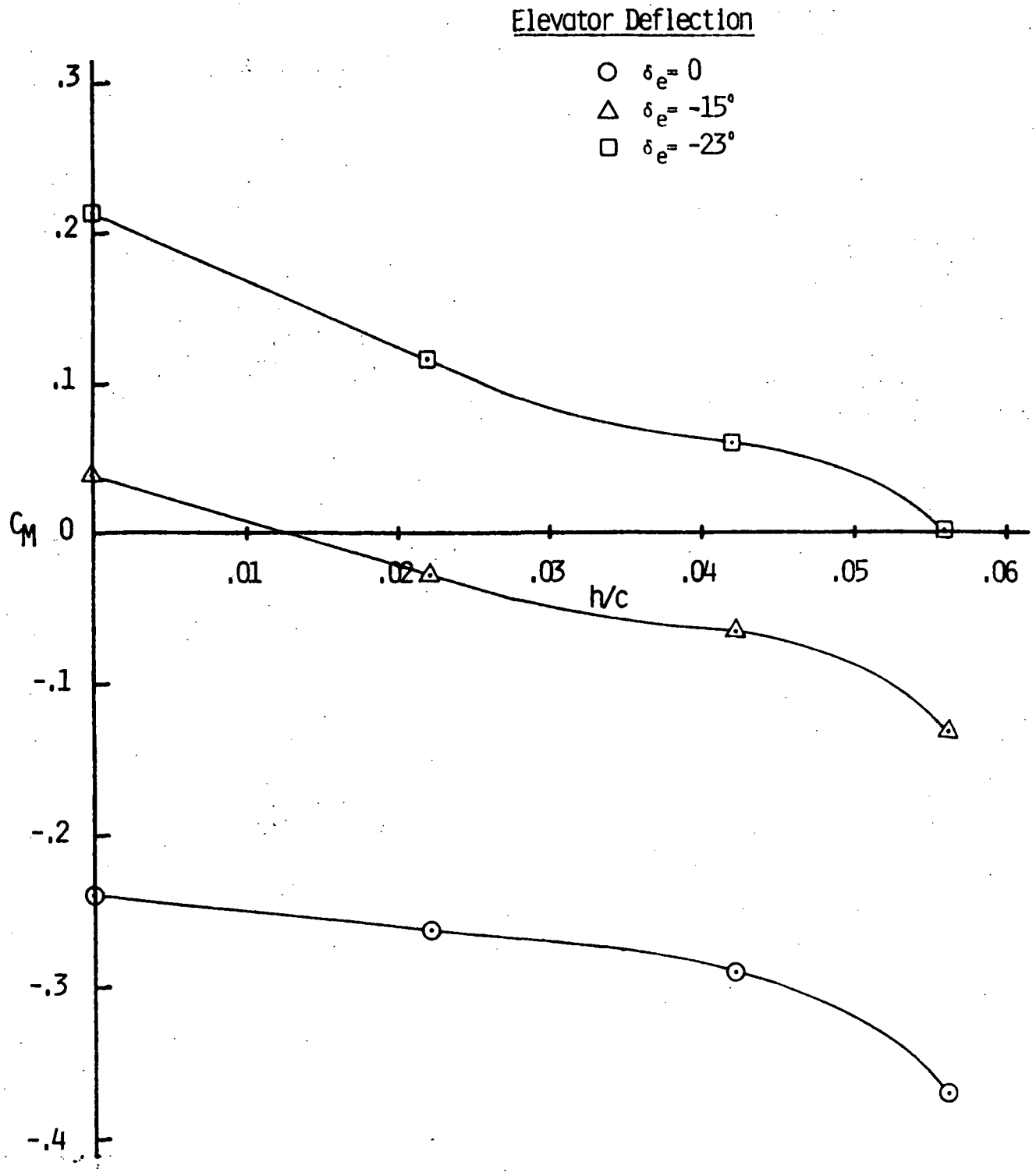

Figure 24. Variation of Pitching Moment Coefficient with Spoiler Height; 77 bhp, 30° Flaps, $\alpha = 10°$

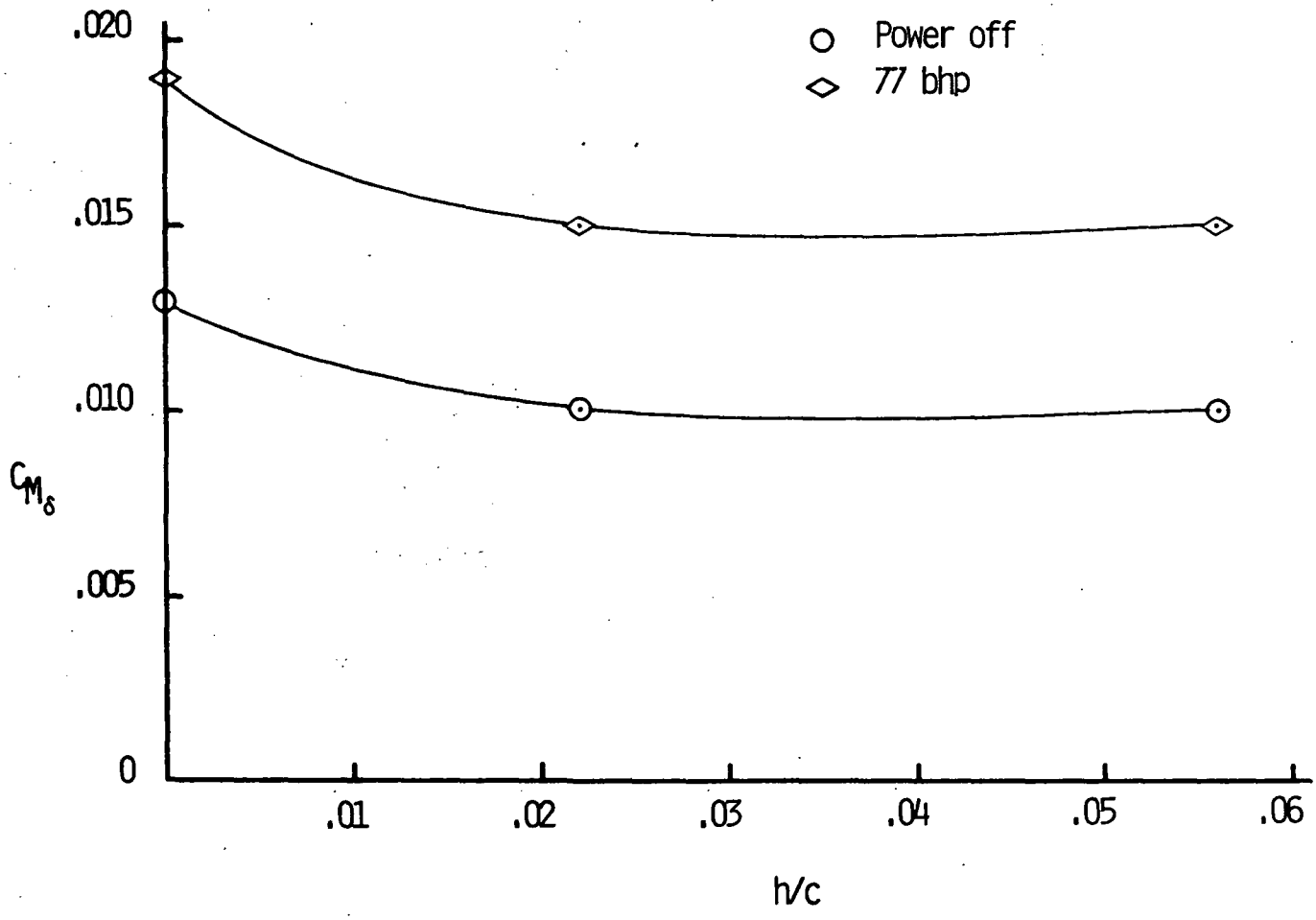

a. With Spoiler Height

Figure 25. Variation of Pitching Moment Coefficient Slope

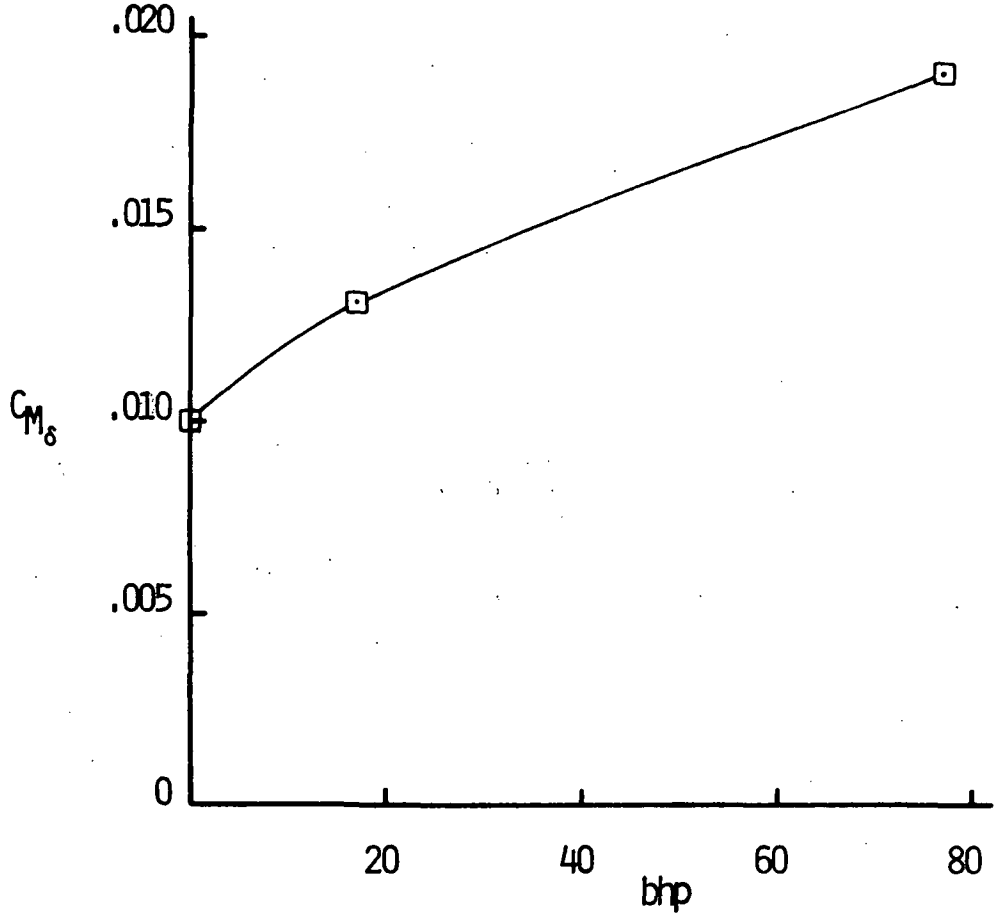

b. With Power

Figure 25. Variation of Pitching Moment Coefficient Slope

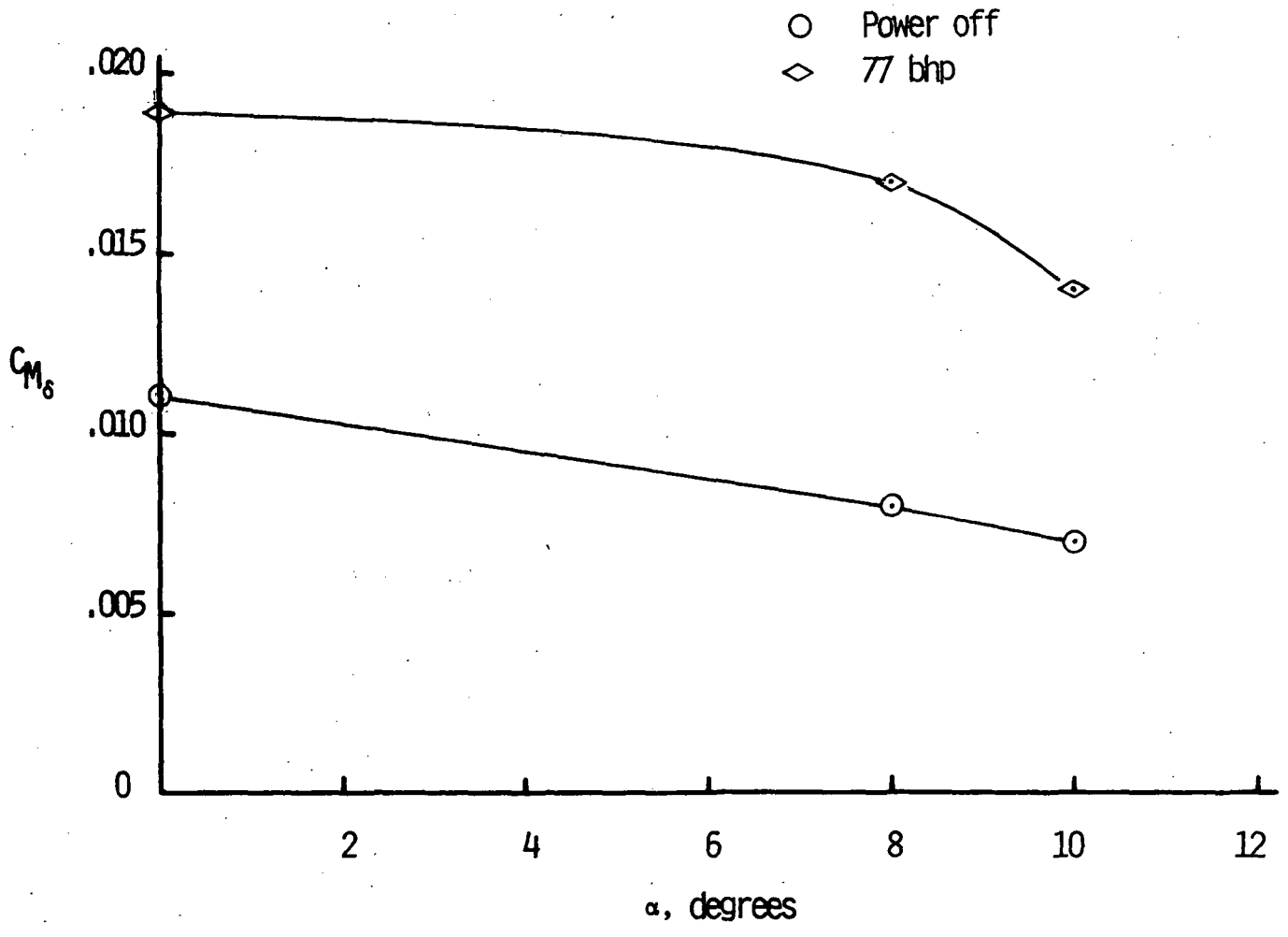

c. With Angle of Attack

Figure 25. Variation of Pitching Moment Coefficient Slope

flaps. This lack of effect is shown in Figure 9.

Thus, the overall effect of the spoiler deploying at high angles of attack would be to reduce the elevator's effectiveness slightly while providing its own negative pitching moment. Attempts to override the spoiler by increasing elevator deflection would result in increasing the spoiler's effectiveness.

This apparent interaction of the elevator and spoiler would tend to invalidate the assumption of independence established in Reference 4 and Equation (1). However, other factors normally ignored in preliminary analysis can have as large or larger effects. Figure 25 shows the changes in $C_{m_{\delta_e}}$ due to h/c, power, and angle of attack for the test aircraft. The parameter having the least effect is h/c. Therefore, within the limits of experimental accuracy, the assumptions of independence can still be considered valid for preliminary design.

Since the changes in C_M due to either elevator or spoiler deflection are assumed to be linear, the interaction effects can be accounted for entirely within the last, or spoiler, term of Equation (1).

Concluding Remarks

The results of theoretical studies, small scale wind tunnel tests, and the full scale aircraft tests in the 30 x 60 foot wind tunnel at NASA Langley Research Center show that the spoiler system can stall proof the aircraft, and the theoretical approach developed in References 3 and 4 is valid. There are still 2 major areas of concern that can be investigated by a flight test or simulator study. They are establishing the maximum usable range of angle of attack and the appropriate change in spoiler height with angle of attack.

Full scale wind tunnel tests have shown that for this particular aircraft, the lift curve at stall is relatively flat and the stall condition does not produce a severe drop-off in lift coefficient. If this occurs in flight, the deployment of the spoiler can be delayed to a higher angle of attack range, allowing the aircraft to be flown closer to its maximum lift coefficient throughout the center of gravity range.

The spoiler deployment rate with angle of attack is based mostly upon engineering experience. This deployment rate will significantly affect the stability characteristics at high angles of attack and in turn produce an increase in stick force. This increase in stick force has been experienced in previous flight tests using the spoiler concept.

The results of further flight tests coupled with the static stability results presented in this report should produce a better understanding of the design requirements for a spoiler system capable

of preventing aircraft stall.

Any future flight test program should include an evaluation of the aircraft handling qualities, which cannot be obtained from wind tunnel tests. Results obtained to date indicate that the spoiler system should provide a significant improvement in handling qualities at high angles of attack.

References

1. Chevalier, Howard L., and Brusse, Joseph C., "A Stall/Spin Prevention Device for General Aviation Aircraft," SAE Paper No. 730333, April 3-6, 1973.

2. Chevalier, Howard L., "Aerodynamic Spoiler for Preventing Airplane Stall/Spin Type Accidents," Final Report No. FAA-RD-75-21, U.S. Department of Transportation, Federal Aviation Administration, December, 1974.

3. Chevalier, H.L., "Some Theoretical Considerations of a Stall Proof Airplane," SAE Paper 0096-736X/80/8803-2096, Volume 88 SAE Transactions, 1980.

4. Chevalier, Howard L., "Wind Tunnel Tests of Aerodynamic Concepts for Stall Proofing a General Aviation Airplane," Interim Report NASA Research Grant NSG-1407, May, 1979.

5. Chevalier, H.L., Wilke, R.A., and Faulkner, M.L., "Wind Tunnel Evaluation of Aerodynamic Spoiler on General Aviation Aircraft Horizontal Tail, Part I," Interim Report NASA Research Grant NSG-1407, May, 1979.

6. Perkins, C.D. and Hage, R.E., "Airplane Performance and Stability," John Wiley and Sons, New York, 1949.

7. Silverstein and Katzoff, "Design Charts for Predicting Downwash Angles and Wake Characteristics Behind Plain and Flapped Wings," NACA TR 648, 1940.